INVESTIGATING THE PRESENT AND FUTURE RISK OF PLUVIAL FLOODING AT HEATHROW AIRPORT, UK, USING A HYDRODYNAMIC MODEL

ALEXANDER BEAVIL

APRIL 2022

Presented as part of, and in accordance with, the requirements for the Final Degree of B.Sc. at the University of Bristol, School of Geographical Sciences, April 2022

University of BRISTOL
School of Geographical Sciences

CERTIFICATION OF OWNERSHIP OF THE COPYRIGHT IN A TYPESCRIPT OR MANUSCRIPT

Dissertation presented as part of, and in accordance with, the requirements for the Final Degree of B.Sc at the University of Bristol, School of Geographical Sciences.

I hereby assert that I own exclusive copyright in the item named below. I give permission to the University of Bristol Library to add this item to its stock and to make it available for use and re-copying by its readers.

AUTHOR	**Alexander Beavil**
TITLE	**INVESTIGATING THE PRESENT AND FUTURE RISK OF PLUVIAL FLOODING AT HEATHROW AIRPORT, UK, USING A HYDRODYNAMIC MODEL**
DATE OF SUBMISSION	**7th April 2022**

Signed: Alexander Beavil
………………………………………………………………………………………………

Full name: Alexander Richard Beavil
………………………………………………………………………………………………

Date: 07/04/2022
………………………………………………………………………………………………

Abstract

The economic impacts of a temporary closure of Heathrow Airport is estimated to be over £23 million a day. The airport is potentially at risk of surface water (pluvial) flooding, in part due to its flat nature and high impermeable surface cover. The intensity and frequency of large rainstorms is anticipated to increase in the future as a result of anthropogenic climate change, which may increase the likelihood of flooding affecting airport operations. In this investigation, the intensity of present and future rainfall events on timescales of 1 to 24 hours were estimated using intensity-duration-frequency curves and future uplift values derived from the UK Climate Predictions 2018 (UKCP18). This rainfall is then applied to a hydrological model, LISFLOOD-FP, to explore the risk that Heathrow and its surrounding infrastructure face from pluvial flooding. The results are then compared with the findings of Heathrow Airport's submissions to the Airports Commission in 2014. The airport is shown to be at low risk of pluvial flooding in the present day, although the risk increases substantially when future uplift is applied. Surface transportation infrastructure, is found to be at most risk under these scenarios. The model appears to provide results similar to those submitted to the Airports Commission, although it is clear that some areas of the airport are reliant on complex managed drainage systems. This study finds that it is likely that the overall drainage capacity will need to be increased in the future, in line with the airport's sustainable drainage assessment.

Word Count: 9981 words

Acknowledgements

I am extremely grateful to my dissertation supervisor Jeff Neal, who has provided extensive support both with the design of the project and the implementation of the modelling, as well as Gemma Coxon, whose guidance on the procurement of rainfall data was extremely helpful. Finally, I would like to thank my friends and family for their consistent support throughout the project.

Table of Contents

List of Tables

List of Figures

1 Introduction

In the UK, over 3 million properties are at risk of surface water flooding (Environment Agency, 2020), causing over £600 million worth of damages each year (Sayers *et al.*, 2020). Anthropogenic climate change is expected to double these costs to more than £1.2 billion annually by 2080, and to bring total annual flooding-related damages above £3 billion (ibid). Understanding areas at risk of flooding is therefore more important than ever, to allow the government, developers and residents to apply appropriate mitigation to reduce their impacts.

On the 12th July 2021, nearly 76mm of rain fell over 90 minutes in parts of London, resulting in pluvial flooding in many parts of the capital (JBA Risk Management, 2021). By midday, eight underground lines were suspended and multiple rail stations (including Euston station, a major long distance terminal) were closed due to flooding. On the 25th July 2021 another storm led to recorded rainfall in excess of 41.8mm over the day, estimated to be between a 1 in 50 and 1 in 100 year event. Large amounts of essential transport infrastructure were left underwater for hours, causing significant travel disruption (Sharman and Burford, 2021). More than anything, July 2021 showed that UK transport infrastructure is simply not ready to deal with the increases in both intensity and frequency of storms that anthropogenic climate change will bring. Pudding Mill DLR station is a good example – the station was completely rebuilt to allow for Crossrail development in 2014 (Smith, 2011), although on the 25th July 2021 the main station concourse was flooded to a depth of 0.5m as a result of intense rainfall in the area. The damages associated with this series of storms are likely in the tens of millions of pounds; as a result of future climate change, the frequency of these events will increase, which will require a significant improvement in the resilience of transportation infrastructure.

In order to assess the risk of flooding to a specific area, one can use a flood model, which allows testing of different scenarios and can assist the development of mitigation measures. This can provide an accurate assessment of risk, which is of particular interest to planners and insurers. It is also essential to the design and operation of essential transport infrastructure, such as airports, motorways and railways, where small amounts of flooding can lead to the potential for loss of life if not managed correctly.

This study uses LISFLOOD-FP (Neal, Schumann and Bates, 2012), a hydrological flood model, to understand the likelihood of surface water flooding in the area around Heathrow Airport both in the present day and in the future. These results are then compared with the findings of similar studies of flooding in the Heathrow area. As one of the largest single pieces of critical infrastructure in the UK, Heathrow provides a good example of the risks that infrastructure may be faced with across the country, both now and in the future.

2 Literature review

2.1 What is pluvial flooding?

Pluvial flooding, also known as surface water flooding, is caused by intense rainfall events that exceed the ability of the ground, vegetation and artificial drainage to absorb the water, leading to surface runoff and ponding. This can be seen on a small scale as puddles on pavements and roads during rain showers, and tends to form at the local elevation minima. Some level of pluvial flooding occurs during all precipitation events, although it tends to be of both limited extent and depth in most well managed areas. The major local factor associated with pluvial flooding is the ability of the ground to absorb water, and its prevalence is strongly dependent on land use and management. Summer convective storms, which lead to intense but short rain showers are the most likely events to cause direct pluvial flooding (Leon *et al.*, 2016). However, in areas where the ground is saturated (such as due to a long event or antecedent rainfall), pluvial flooding can occur as a result of low intensity but longer duration winter storms. Thick vegetation cover tends to intercept the majority of the rainfall that occurs in short duration showers, which reduces the effective precipitation rate at the surface. In urban areas particularly, this cover does not exist. The higher water input is also compounded by a high prevalence of impermeable surfaces - such as asphalt and concrete - which convert all incident precipitation into runoff, and have a very low storage capacity. This runoff tends to collect at the local elevation minima , resulting in the formation of deep puddles that can approach the scale of lakes, which can cause major issues if important infrastructure or property exists in these areas.

The cost of flooding can be assessed both in terms of physical damage, as well as economic damage from lost revenue and capabilities. Airports are a good example of locations where flooding tends not to cause much physical damage, although it has the potential to cause major economic damage, both directly to the airport and its airlines, and indirectly through its and impacts on business and travel. Airports contain large areas of flat, impermeable surfaces in the form of runways, taxiways, roads and car parks. Due to the extensive connectivity associated with their operation, they are also extremely vulnerable to disruptions to surface transportation in the local area, usually in the form of the surrounding roads and motorways. This, in theory means that there is a potential for pluvial flooding to affect operations both on the airport and in its local network where proper mitigation has not been applied, maintained or has failed.

2.2 Why does Heathrow Matter?

Heathrow Airport, located to the west of London is the UK's busiest airport, handling over 280 000 flights and 80 million passengers in 2019 (CAA, 2020a). Perhaps more importantly it is also the busiest international freight hub, and handled 1.5 million tonnes of freight in the same year. The suspension of transatlantic flights due to COVID-19 restrictions was estimated by Heathrow Airport Limited (HAL) to cost over £23 million a day (BBC News, 2021) – widespread flooding would likely lead to far higher costs. The huge scale of the airport means that any disruption that occurs there has immense repercussions that extend far outside the airport's perimeter.

The area surrounding Heathrow Airport is underlaid by a shallow aquifer formed of 3-6m of Terrace Gravels, which are very permeable (AMEC, 2014a, p. 6). This layer sits above a layer of impermeable London Clay over 50m thick, which leads to the groundwater levels being less than 2m below the surface in normal circumstances. This can lead to regions of surface saturation, and thus very low infiltration rates. In addition, particularly to the northwest of the airport, a large area of present and past sealed landfill exists (AMEC, 2014a, p. 9), which disrupts the flow of water in the aquifer, as well as increasing runoff at the surface. The airport itself contains large numbers of impermeable surfaces, in the form of car parks, roads, buildings and aircraft aprons/taxiways/runways. The latter category are supported by extensive drainage systems designed to keep surface ponding to an absolute minimum.

For aircraft operations, the maximum level of standing water permitted is very low, with runways being defined as *contaminated* when standing water depth exceeds 3mm over more than 1/3rd of the runway. This value is significantly lower than the usual 10 or 20cm of permitted flooding in urban areas. This low boundary does specifically only apply to runways, although aircraft operations would likely be significantly impaired if water levels exceed 10cm anywhere on the aerodrome. This makes the airport an obvious location where small amounts of pluvial flooding could cause significant disruption, and thus an ideal candidate for further assessment.

2.3 Reports concerning the flood risk at Heathrow

Over the last two decades, a wide variety of reports have been commissioned looking into the flood risk at Heathrow Airport, and particularly the effect of the airport on the flood risk of the surrounding area. The airport has been trying to make the case for the construction of a third runway, usually directly north of terminal 5. The government set up an independent body – The Airports Commission (AC)– chaired by Sir Howard Davies "to identify and recommend to government options for maintaining the UK's status as a global aviation hub" (Graham, 2013). HALs, the current operator of Heathrow commissioned AMEC consultancy to prepare evidence for the AC, which was published in June 2014 (AMEC, 2014a, 2014b, 2014c). Later in the year, Jacobs UK (another consultancy) produced a similar report independently looking at the various proposals submitted to the AC by different stakeholders. Their report (Jacobs UK, 2014) was published in November 2014. This report contains a more detailed look at the pluvial flood risk using the surface water risk map published by the Environment Agency (EA), although does not perform any modelling of its own. The final report published by the AC in July 2015 makes very little reference to the flood risk at any of these sites, but recommends that a third runway should be constructed in line with HAL's proposal.

2.4 Modelling floods

A number of different approaches to modelling floods exist, using different technology and resources. Initial modelling efforts focused on the construction of large physical models, which provided a good understanding of some of the processes at play in the development and retreat of floods. More recently with the advent of advanced computing techniques, flood modelling has become more focused on numerical models (Bates *et al.*, 2005). This is substantially cheaper than building and operating large physical models, which has allowed the amount of modelling studies to increase substantially. The most common type of numerical method is a hydrodynamic model, which use an understanding of physical processes to apply mathematical equations that represent fluid flow. AMEC (2014a) also used a hydrodynamic model (TUFLOW) in their flood risk assessment for the local area. Their Lower Colne Valley integrated flood model works over two dimensions in the floodplain, and uses one dimensional channel flow. This is similar to the approach taken by LISFLOOD-FP, described in the following section.

2.5 LISFLOOD-FP

2.5.1 What is it?

LISFLOOD-FP is a raster based hydrodynamic model that uses regular storage cells to produce extent and depth predictions using simplified floodplain hydraulics (Bates and De Roo, 2000). Throughout its over 20 year history, LISFLOOD-FP has had a large number of improvements and additions, to add new features as well as improve computational efficiency and its modelling performance. The model was used in the early 2000s for a number of different studies (e.g. Horritt and Bates, 2002; van der Sande, de Jong and de Roo, 2003), where its simplicity and low computational cost was a great asset. As a raster based model, water is contained within a series of cells of pre-defined size. It is then able to flow between cell margins, with the rate and direction of transfer being governed by a series of mathematical equations. A wide variety of different methods ('solvers') exist to do this, and provide different methods for parameterising floodplain and channel flow.

2.5.2 Acceleration Solver

The acceleration solver is a two dimensional mode method used by LISFLOOD-FP for deep water on floodplains. It solves a reduced complexity version of the Saint Vernant equations that assume convective acceleration is negligible. The model uses two equations to handle continuity of mass in each cell and the continuity of momentum between cells as described in Neal *et al*. (2012). For each cell, the continuity of mass over time step Δt is described by

$$h_{i,j}^{t+\Delta t} = h_{i,j}^{t} + \Delta t \frac{Q_{x\, i-\frac{1}{2}j}^{t+\Delta t} - Q_{x\, i+\frac{1}{2}j}^{t+\Delta t} + Q_{y\, i-\frac{1}{2}j}^{t+\Delta t} - Q_{y\, i+\frac{1}{2}j}^{t+\Delta t}}{A_{i,j}} \tag{1}$$

Where Q is the flow between cells, h is the water depth at the centre of each cell, A is the cell surface area and subscript i and j are the cell spatial indices in the x and y planes. The momentum equation operates along each cell face as a one dimensional operation such that each cell face operates independently. For each of the x and y planes, the momentum equation to calculate flow Q between two cells is described by

$$Q_{i+\frac{1}{2}}^{t+\Delta t} = \frac{q_{i+1/2}^{t} - g h_{flow}^{t} \Delta t S_{i+1/2}^{t}}{\left[1 + g \Delta t n^2 \left|q_{i+1/2}^{t}\right| / \left(h_{flow}^{t}\right)^{\frac{7}{3}}\right]} x \tag{2}$$

Where Δx is the cell width, g is the acceleration due to gravity, q^t is the flow from the previous timestep Q^t divided by the cell width x, S is the water surface slope between cells, n is the Manning's roughness coefficient and h_{flow} is the depth between cells through which water can flow. In order to maintain model stability,

$$\Delta t \propto x \tag{3}$$

$$\Delta t \propto \frac{1}{\sqrt{max(h^t)}} \tag{4}$$

Where $max(h^t)$ is the maximum water depth in the model domain. The timestep equation is based on the Courant-Freidrichs-Lewy condition. This provides a significant improvement to computational cost compared to the previous diffusive solver, where the timestep scales directly with maximum water depth, and thus can become very small (Bates, Horritt and Fewtrell, 2010).

2.5.3 Routing Solver

The Acceleration solver struggles to handle terrain discontinuities, including steep slopes, roofs and walls; these features can lead to instability as they violate the long-wave, small vertical velocity assumption of the shallow water equations. There are also questions to be raised as to whether the shallow water equations provide good approximations in very shallow (<3mm) depths of water. The Routing solver (Sampson *et al.*, 2013) is an addition to the standard acceleration solver, designed to address these problems in areas where very shallow water is present. Under these conditions, the flux of water between cells is defined by the lowest of the four neighbour cells. If no lower neighbour is present, the cell is identified as a 'no-routing' cell, which leads to accumulation; once water accumulates above the depth threshold, the Acceleration solver is used, allowing water flow in any direction. The rate of flow of water is dependent on the difference in cell elevation as well as inundation depth, to avoid water being transported upslope. The timestep in which this occurs is fixed, to avoid unrealistically high velocities. This method provides the best of both worlds, and ensures that the model remains stable under even the most intense rainfall. It also provides an ~25% improvement in model runtime with no obvious drop in performance, as the computationally expensive hydraulic equations are not used on all cells.

2.6 Rainfall data

Extreme rainfall events are the usual cause of pluvial flooding. Identifying the magnitude and return period of these extreme events is challenging, particularly when considering events with return periods of 100 or 1000 years. One major reason is that there is a large amount of both interannual and decadal variability in rainfall, particularly in the UK. Intense rainfall events tend to be associated with convective storms, which usually (although not exclusively) occur in the summer months (Leon *et al.*, 2016). These storms form along convergence lines – areas of air that remain laterally stationary – which leads to large amounts of precipitation over a small area. A storm of this type in Boscastle, Devon in 2004 resulted in more than 82mm precipitation being recorded over 1 hour, and 148mm over 3 hours (Golding, Clark and May, 2005). These events are relatively infrequent in the UK, which means that long time series data are required to identify them, and makes assessing their frequency rather difficult.

The most intense rainfall events occur over short durations, which means that a high frequency of data collection is essential to identify them. The highest frequency rainfall timeseries available for the UK is at a 15 minute interval, although this is currently only available for a short (<10 year) period for locations near the study site (e.g. Environment Agency, 2021b), or does not include recent data (e.g. Met Office, 2022). Lewis *et al*. (2018) developed a 1km resolution rainfall timeseries for the period 1990-2015 (later extended in Lewis *et al.* (2022) to 1990-2017) that uses hourly rain gauge data from 1900+ stations to provide full coverage of the UK. The dataset primarily uses tipping bucket rain gauges, which are known to under-record at high rain rates, as well as during high wind (Golding, Clark and May, 2005). For quality control purposes, this data was compared to the daily totals, with suspect station results removed from the resulting product.

2.6.1 Intensity-duration-frequency analysis

A relationship exists between the intensity of rainfall, duration and return period, which is commonly represented using an intensity-duration-frequency curve. Many different methods exist for creating these curves, and different methods are preferred depending on usage, data availability and computational cost. One simple method is to use a Generalised Extreme Value Distribution (GEV), which is based on extreme value theory's (EVT) description of the tail of probability distributions, which allows for the estimation of rare and unobserved events (Ulrich *et al.*, 2020). A detailed description of this method is included in Ulrich *et al*. (2020), although for the purposes of this study only hourly duration rainfall data was used, rather than a combination of different statistical periods, which simplifies the method. GEV provides a framework for the extrapolation of rainfall events based on the EVT, although it remains vulnerable to the issues associated with out-of-sample analysis. This means that the accuracy of the values provided is in reality unknown as they were not observed, and may act differently to the range used.

2.7 Climate change

As a result of anthropogenic climate change, it is expected that the hydrological cycle will intensify, leading to an increased risk of flooding and drought across the world (Watts *et al.*, 2015). The strength of this increase is currently unclear, and depends as much on the emissions pathway taken as the science. The UK Climate Projections 2018 (UKCP18) are the latest assessment of climate variability and expected future change produced by the Met Office (Lowe *et al.*, 2018), and focus on how climate in the UK may change over the next century. Major improvements were made through the use of an ensemble of more recent models compared to the previous UKCP product produced in 2009, including the simulation of natural interannual variability, and more comprehensive observational constraints. These predictions show that irrespective of the emissions pathway taken, an increase in the intensity and frequency of high rainfall storms will occur, with a larger increase for higher emissions scenarios.

2.8 Infiltration

The rate of infiltration is important to understanding the pluvial flood risk at the surface. In areas with high infiltration rates pluvial flooding is unlikely (but not impossible), as the water is likely to drain away. The effective infiltration rate (EIR) of any one point is dependent on the soil type and underlying geology, artificial drainage and land cover. Including drainage and interception in the infiltration rate (to form EIR) is one of the most common methods of dealing with these factors, with the alternative option being to remove these rates from the input precipitation. The latter method is non-ideal, as it would require a spatially varying rainfall rate, although the effects are similar.

2.8.1 Land cover

The surface cover of a location is extremely important to understanding its EIR. In zones with dense forest cover, interception of precipitation is likely to occur, with much of the water not making it to the surface on a short timescale. This is not strictly infiltration of the water as it still remains above the surface, although it is included in EIR here for simplicity. Urban areas, and particularly the airport contain a high proportion of sealed surfaces, consisting of buildings, asphalt and concrete. These surfaces are (mostly) impermeable, and thus have an infiltration rate of near zero. In order to convert a land cover map to its effect on infiltration rates, an approximation of the amount of sealed surfaces and interception that will occur is required, such as the one produced by Pauleit and Duhme (2000).

2.8.2 Soils

Soil type is an essential factor in determining the infiltration rate at a location. The ground conditions around Heathrow are of particular interest to this study, due to the thick layer of impermeable London Clay located between 3 and 6m below the surface, as well as high groundwater levels throughout (AMEC, 2014a). There is a large amount of variation in the thickness and composition of the Taplow Gravels that overlay the clay, naturally and due to past extraction for construction (AMEC, 2014b).

2.8.3 Drainage

Drainage is present in most urban areas, usually in the form of combined or storm drains. Its main purpose is to mitigate against the effects of sealed surfaces, and ensure that surface water flooding does not occur. Due to the complex nature of drainage arrangements, it is impossible to include them all in reasonable pluvial flood model; instead they are parameterised. The most common method when specific drainage arrangements are not known is to use a spatially consistent drainage rate, which can then be included in the model as part of the EIR. The scale of drainage arrangements vary, although it is most likely to be of high capacity on and around Heathrow Airport, due to its importance. The Environment agency recommends a standard drainage rate of 12mm/hr for most urban areas, with an upper bound of 24mm/hr for important infrastructure assets (Environment Agency, 2019). This is almost certain to be an underestimate of the drainage capabilities of the runways and taxiways of the airport, but provides a suitable approximation for other areas. Drainage is only applied to areas marked as urban or suburban land cover. The resulting spatially dependent drainage layer is applied as part of the EIR to the flood model.

2.9 Measuring flood impacts

The impacts that a flood event has depend on the extent of flooding, as well as its depth. The depth at which a flood causes significant impacts depends on the land use. The UK Civil Aviation Authority (CAA) defines a runway with standing water more than 3mm deep as “contaminated” (CAA, 2020b). This extremely low threshold exists as aircraft operating at high speed on the runway are vulnerable to hydroplaning, which can impair directional control and braking. Aircraft operations can be permitted above this depth, although they are restricted as braking distances can be up to 3 times higher than usual. An exact value for the highest water depth that would still allow operation of the runway is not published, as it would depend on breaking tests performed using Continuous Friction Measurement Equipment. For this study, a value of 10mm was chosen as the highest value that would be likely to permit aircraft operations. This also accounts for the fact that the Heathrow runways are grooved to a depth of 5mm, which would result in the effective water depth being lower (around 5mm).

Pregnolato *et al*. (2017) reviewed a wide variety of studies looking at the impact of flooding on road transportation. They produced a depth-disruption curve, and found that at a depth of 10cm, road speeds are reduced by up to 50% (Pregnolato *et al.*, 2017). This would lead to significant disruption, particularly on the motorways and access roads that surround the airport. They also found that most smaller vehicles would be at risk of stalling due to water filling the air intakes at a depth of 20cm. The environment agency reported that flooding in the depth range 15-30cm would lead to property flooding in some areas, as well as causing damage to exterior walls (Environment Agency, 2019, p. 26).

In the field of risk management, events are classified by comparing their likelihood and severity, and forming a composite risk index (Naso *et al.*, 2016). This provides a useful, albeit subjective framework for comparing different hazards. In a similar vein, it is possible to assess flood hazards by their extent and depth. Deeper events cause more destruction in a localised area, although larger extents can also lead to significant physical and economic damage. This study uses a *flood score* index to compare events based on their depth and extent, to allow for comparison between events that are likely to cause a similar level of disruption and damage.

Figure 1: Regional map of model domain (shown in black rectangle); base map ESRI Standard.

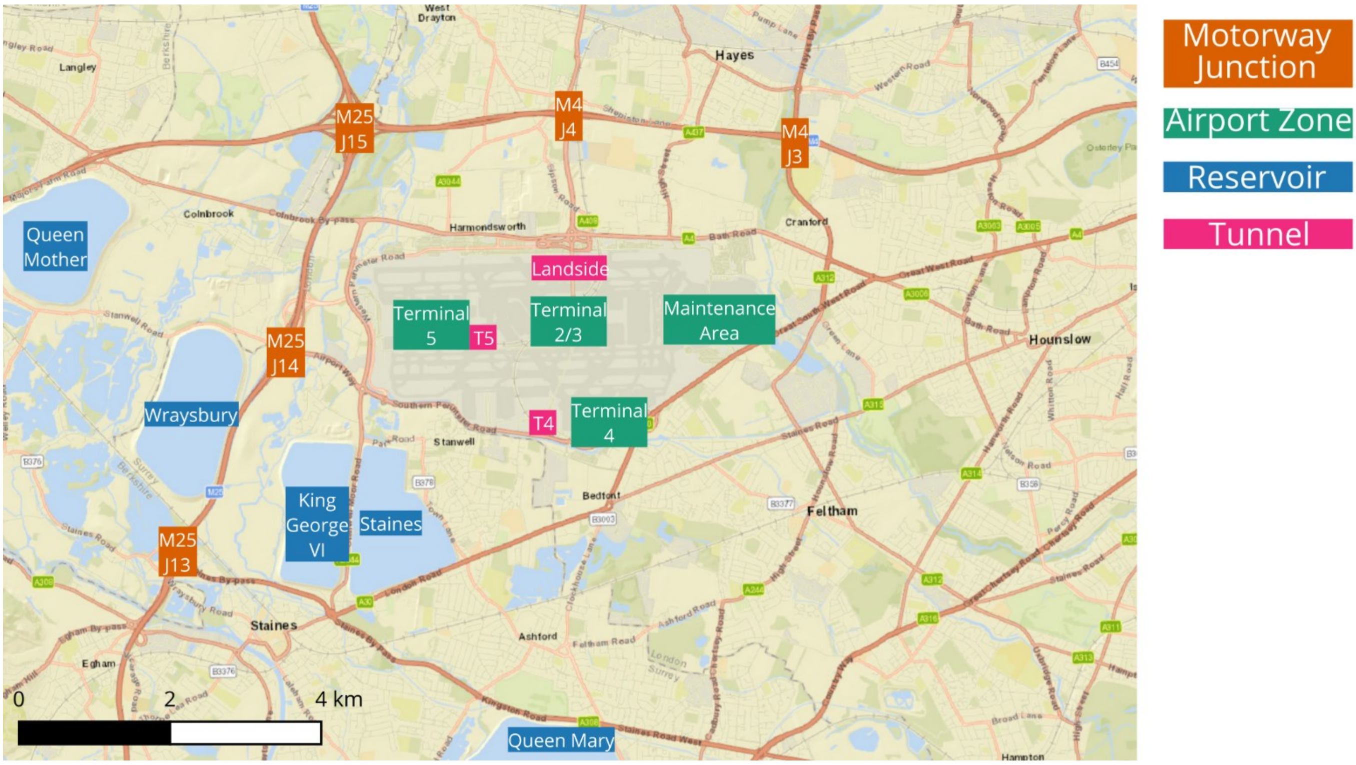

Figure 2: Map of model domain, showing points of interest; base map ESRI Standard.

Figure 3: Map of model domain, showing LiDAR elevation derived from EA (2021a). See section 3.5 for details.

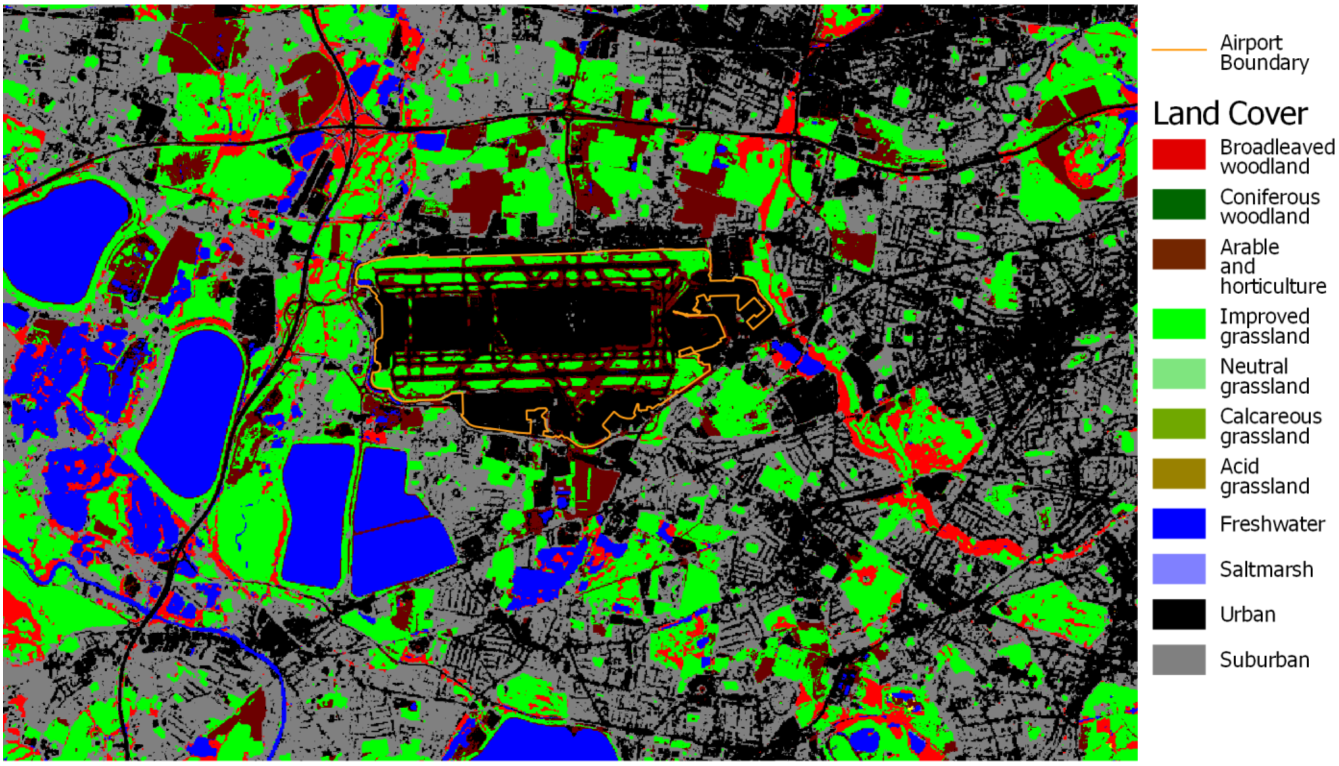

Figure 4: Map of model domain, showing land cover derived from Morton *et al*. (2021). See section 3.6.3 for details.

2.10 Site Selection

As the largest airport in the UK, Heathrow provides the ideal location to investigate the risk of pluvial flooding on airports. Figure 1 shows the location of the airport, to the west of London. Figures 2-4 show the study area in more depth, a 15x10km region around the airport, with points of interest (figure 2), elevation (figure 3) and land cover (figure 4) overlayed. The airport is surrounded to the north, east and south by urban areas, and to the west by a mix of semi-rural and suburban areas. Additionally, to the west are a number of drinking water reservoirs, as well as a floodplain/marsh area associated with the Rivers Colne and Thames. The area surrounding these reservoirs contains flooded pits formed as a result of quarrying for clay. The Airport property itself takes up a 9.5km^2 area in the centre of the study area, shown in orange on figure 3. This covers all areas classified as “airside” (including all areas where aircraft would operate), although it excludes some of the British Airways maintenance area at the east end of the airport, which would not usually be essential to airport operations. A number of other landside areas would also be essential to the operation of the airport, or rather, the movement of passengers and freight in and out of the airport. These include the direct approaches to each of the terminals, the landside tunnel to terminals 2 and 3 as well as the approach roads. The airport is accessed from the motorway network at M25 J14 (Terminals 4 & 5) and M4 J4 (Terminals 2 & 3), with the M4-M25 interchange at M25 J15 providing connectivity to the rest of the country. The high density of complex transport infrastructure in the area provide an interesting set of modelling challenges, as well as a number of bottlenecks where flooding could create significant disruption.

2.11 Sensitivity studies

In order to assess the usefulness of a model, an understanding of its sensitivity to the boundary and initial conditions is essential. A hydraulic model contains a large number of parameters that can impact its outputs. The rainfall event and EIR are the clearest components with which the model is likely to be sensitive when considering only pluvial events. A wide variety of rainfall events are thus useful to test, particularly to test the hypothesis that only short duration events are likely to provide significant flooding. EIR is another important factor – due to computational and time constraints it is unfortunately not possible to test as wide of a variety of scenarios as for rainfall. Drainage was identified as the largest uncertainty, as it forms the majority of the EIR around the airport (as most of the airport is classified as urban/suburban, and thus has a low background infiltration rate).

2.12 Aims and Objectives

This study aims to assess the likelihood of significant surface water flooding impacting the operation of Heathrow Airport, both now and in the future. In order to achieve this, it will:

- Use various rainfall data sources to perform an intensity-duration-frequency analysis of rainfall at the study site both in the present day and future as a result of anthropogenic climate change.
- Run an ensemble of LISFLOOD-FP simulations with varying rainfall and drainage values, and assess the sensitivity of the model to the drainage parameterisation.
- Assess the risk of pluvial flooding to the surface transport network in the area surrounding Heathrow on airport operations and identify areas at particular risk both in the present day and future.
- Compare the model results here with the various reports produced for the AC relating to the local flood risk.

3 Methods

3.1 Model Selection

This study uses LISFLOOD-FP, a hydraulic model described in detail in section 2.5. In this instance, the model uses the routing solver with water depths below 0.3cm, and the acceleration solver in deeper waters. The Manning's friction coefficient is set to 0.04, as used by Sampson *et al*. (2013)

3.2 Rainfall data selection

Rainfall events that are likely to cause high pluvial flooding tend to be those with high intensity, and correspondingly a short duration. In order to capture these events a higher temporal resolution for the rainfall data is thus preferred, whilst also maintaining a long timeseries to capture the extreme events. As such, the CEH-GEAR1hr dataset (Lewis *et al.*, 2019) published by the *UK Centre for Ecology & Hydrology (CEH)* was chosen, which contains hourly gridded estimates for areal rainfall over Great Britain over the period 1990-2014. Additionally, CEH published a more recent version of this dataset that also includes the period 2015-2016 (Lewis *et al.,* 2022), which has been included in as part of an expanded 1990-2016 range.

3.3 Rainfall Uplift

Rainfall uplift values due to anthropogenic climate change have been used to provide an example of what the flood risk might look like by 2070. A derived future uplift dataset from the *UKCP18 Convection Permitting Model projections* (Met Office Hadley Centre, 2019) was used, based on the Representative Concentration Pathway (RCP) 8.5 scenario.

3.4 Intensity-frequency-duration analysis

The "IDF" R Package (Ulrich *et al.*, 2022) is used to generate IDF curves for precipitation events with a duration of 1, 2, 3, 6, 12 and 24 hours using the hourly rainfall dataset at return periods of 2, 30, 100 and 1000 years. The intensity of longer return period events are likely to be overestimated as this method requires a high level of extrapolation. Therefore, although 1000 year return period events are calculated, they are not used as inputs to the flood model.

3.5 Digital elevation model (DEM)

A composite Digital Terrain Model (DTM), derived from airborne laser altimetry (LiDAR) data at a 1m resolution was used for this study (Environment Agency, 2021a). This layer has buildings, trees and other artefacts removed, and is designed to approximate the terrain height. Whilst a DEM that included buildings may have been useful in some cases, limited coverage of the Heathrow Area exists at high resolution. This DTM was reprojected using the GDAL bilinear method to generate a DEM at 10m resolution for use by LISFLOOD-FP; The resultant layer is shown in figure 3. In general, as grid size decreases, computational cost increases quadratically as a result of a need to reduce the model time step to maintain stability (Hunter *et al.*, 2005). A grid size of 10m was chosen to ensure that the model is able to resolve small scale features, such as the edges of taxiways and tunnel entrances, whilst still maintaining a manageable computational cost. The model was configured to allow water to freely drain over the edges of the model domain, although a conversion fault lead to this not occurring along the eastern edge. This issue is described in more detail in section 4.3.

3.6 Infiltration rates

The infiltration layers used are formed of a composite of a number of different datasets, each of which can be varied independently. This effective infiltration rate is thus formed of:

$$I_{soil}C + D \tag{4}$$

where I_{soil} is the soil infiltration rate, C is the sealed surface percentage and D is the drainage rate.

3.6.1 Soil type

The local surface soil type was interpolated using percentage clay, silt and sand samples from the World Soil Information Service's soil profile dataset (Batjes *et al.*, 2017), using the September 2019 snapshot.. Five sample values from within 10km of the airport were averaged to provide an overall classification of the soil type using a soil classification triangle. This resulted in the classification of *Sandy Loam*. The result sits near to the boundary with *Loam*, which is used as an additional classification for sensitivity purposes. . Infiltration rate varies by slope – this was calculated using the 1m resolution LiDAR DEM, before being rescaled using the GDAL median method to provide a slope grid at 10m resolution. An soil-infiltration rate table produced by the US Department of Agriculture (Sacramento County, 1990) was then used to provide an infiltration rate in mm/hr. The infiltration values are shown in table 1.

Slope	**0-4%**	**4-8%**	**8-12%**	**12-16%**	**16+%**
Sandy Loam	19.05	15.24	11.43	7.62	4.826
Loam	13.716	10.922	8.382	5.588	3.556

Table 1: Soil infiltration rate in mm/hr for the relevant soil types. Slope is shown in percentage. Sourced from the Sacramento County Code (1990).

3.6.2 Drainage

Following the standards presented by the EA (2019), drainage has been provided at a rate of 0, 12 and 24 mm/hr for grid cells that are defined to be either urban or suburban. This drainage value is then added to the base infiltration value to provide an overall water removal per grid cell value.

3.6.3 Land cover

Land cover data is used for approximating the amount of sealed surfaces present in each grid cell. A 10m classified pixel dataset (Morton *et al.*, 2021) showing land cover for 2020 was used, and is shown in figure 4. Seasonal composite imagery representing the median surface reflectivity was classified using a random forest, with additional context data (such as height, slope, coastal proximity and urban proximity) used to reduce confusion. This was then validated using known land cover parcels to give confidence values for each cell.

3.7 Experiments

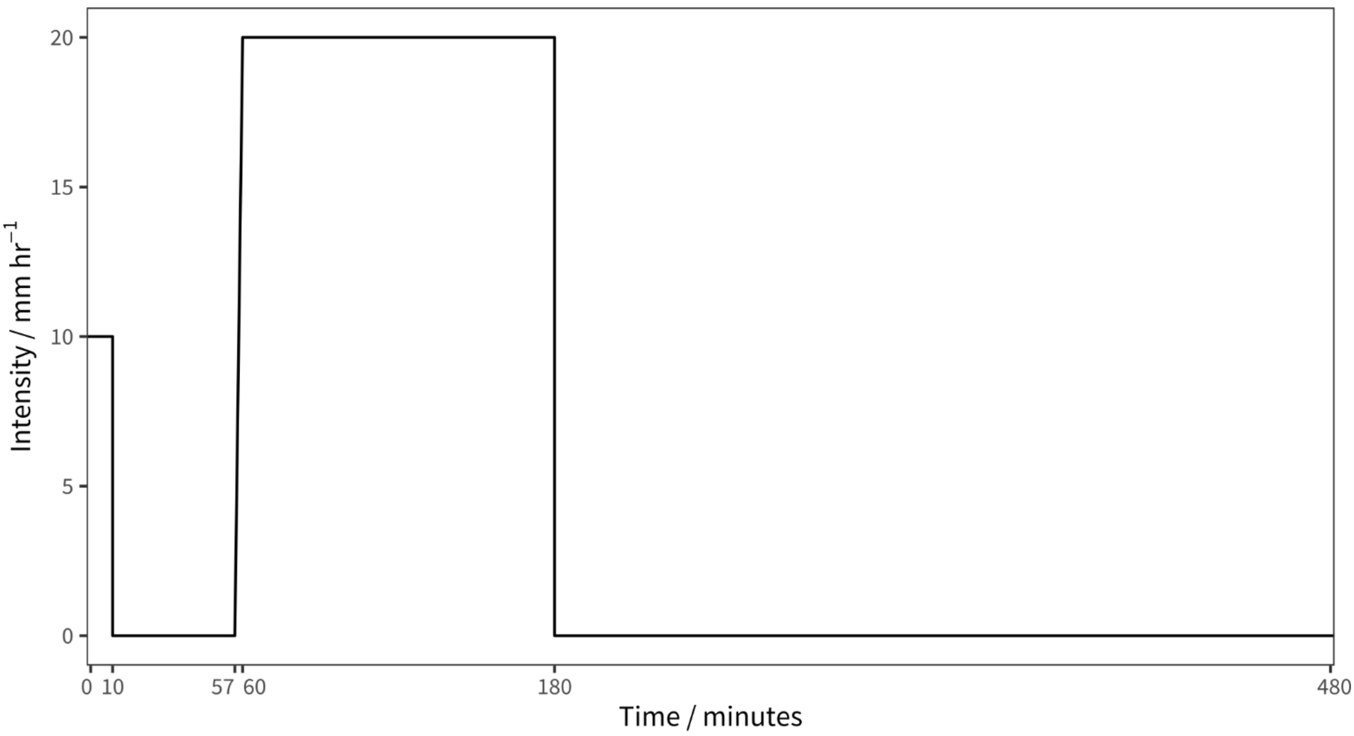

Figure 5: Chart showing incident rainfall intensity for a generic 2 hour rainfall experiment. A 1 hour runup period precedes the main rainfall event, and is followed by a 5 hour period of no rainfall to allow for equilibration.

Each model experiment consists of a combination of a rainfall scheme, a DEM and an infiltration layer. The DEM is common between all experiments, with the infiltration layer being common for all standard experiments. The rainfall scheme consists of a one hour spin up period, a rainfall period and an equilibration period, following the example shown in figure 5. The runup period exists to ensure that holes in the DEM (such as the steep drops seen at the airside tunnels) are wetted at the beginning of the simulation. It also allows the model timestep to stabilise before the main rainfall period is applied. The intensity of this rainfall is 10mm/hr, except during events with less than 15mm/hr intensity, where it is 5mm/hr. This is then followed by a 47 minute quiet period, during which time the rainfall applied will drain away in almost all locations. The main rainfall is preceded by a 3 minute period where the intensity of the rainfall is linearly increased. This ensures that the model remains stable by allowing the timestep to decrease as required. Rainfall is then applied at the defined intensity and duration (see table 3 for details). At the end of this period rainfall ceases, and the model continues for 5 hours with no further rainfall to allow for equilibration and drainage of the water to occur.

3.8 Flood Assessment

Identifier	Depth	Context
0	<0.3cm	No flooding recorded
1	<1cm	Runway operations affected due to hydroplane risk
2	<10cm	Some disruption to traffic flow, runways likely closed
3	<20cm	Significant disruption to traffic, limited property flooding, maximum extent for aircraft operation
4	<100cm	Large scale property flooding, vehicles floating away
5	>100cm	Unlikely to occur, suggests modelling errors

Table 2: Flood water depth definitions used to for classification of model outputs.

A spatial raster containing the maximum water depth is exported from LISFLOOD-FP at the end of each experiment. This is then reclassified using the depths shown in table 2; the area of each depth category is calculated by counting the number of cells in each class. Depths above 100cm are not likely to occur in this domain purely as a result of pluvial flooding. Their presence suggests modelling errors or oversights. The most likely cause is the presence of a tunnel entrance or gap in the DEM data.

In order to compare the magnitude of flooding that occurs in each event, a flood score is calculated. This follows the principles of risk management; the most damaging floods are those with high depths or large extent. The shorter duration events used in this study are of higher intensity – one would therefore expect that the average depth of flooded terrain to be higher, although the extent of flooding to be more limited as a result of a lack of time for equalisation. The converse is true of the longer duration events – here, water has more opportunity to runoff and congregate, and the increased infiltration of incident water will reduce the depth that is possible. Flood score is thus a useful measure to compare events irrespective of duration. It has been calculated using the formula:

$$score = A_{1cm} + 2A_{10cm} + 3A_{20cm} + 4A_{100cm} + 5A_{\infty} \tag{5}$$

Where A is the non-cumulative area of each flood depth category. The maximum flood score is 750, where the entire model domain had a depth of greater than 100cm. This would be impossible, as water would flow over the edge of the model domain before reaching this point.

3.9 Sensitivity analysis

Understanding the sensitivity of the model to change in the boundary condition is essential to determining how useful the results are. This study has chosen to only look at the sensitivity of the model to the drainage rate applied. The main areas of interest have land use classified as urban or suburban, and therefore have drainage applied at a rate which dwarfs the infiltration rate (2:1 for an urban area with low slope, higher in areas with slope).

4 Results

4.1 Rainfall

Figure 6 shows that over the period 1990-2020 a variety of storms were recorded at Heathrow that resulted in intense precipitation. The most intense rainfall recorded was on the 20th July 1992, peaking at 29.4mm/hr between 19:00 and 20:00 UTC. Coincidentally, the second most intense rainfall was recorded on the 20th July 2007 at 22.4mm/hr. There were only 5 days in this time period with rainfall intensity above 20mm/hr, and only 30 above 10mm/hr. In the last decade of the dataset only one day recorded a peak rainfall intensity over 9mm/hr (28th June 2014, 11.2mm/hr); all events over 14mm/hr intensity were recorded before 2008. 38 of the 50 highest intensity rainfall days in this period occurred during the summer months (June to August), with the others occurring in September-November.

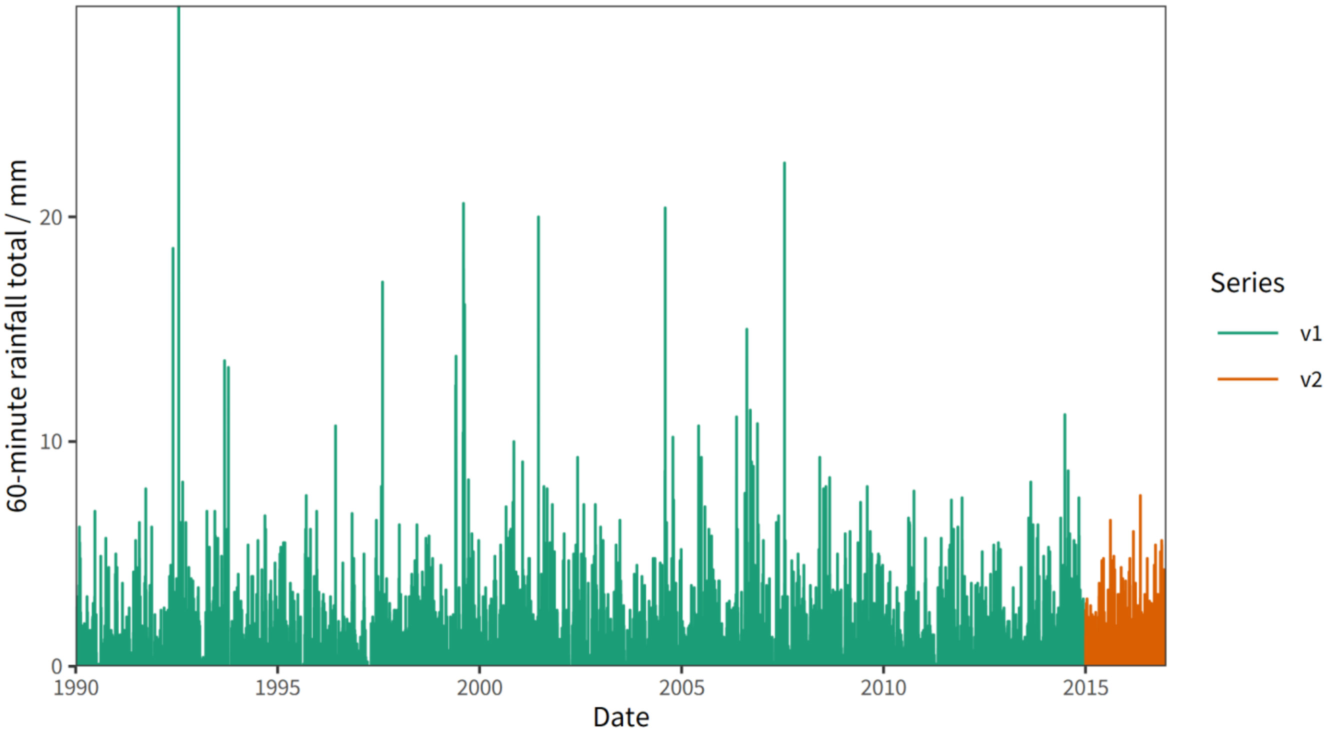

Figure 6: Maximum 60-minute rainfall recorded each week for the Heathrow grid cell from 1990 to 2017. *v1* derived from Lewis *et al*. (2019); *v2* derived from Lewis *et al*. (2022).

The maximum annual rainfall intensity for each year between 1990-2015 (shown in figure 7) clearly shows that the intensity of a rainfall event tends to decrease with an increase in duration. During the study period the highest return period event recorded sits in the 1 in 30 year region for 1 and 2 hour events, and around 1 in 20 for longer events. Thus, the 1 in 100 year rainfall events used in this study requires extensive extrapolation. The addition of 2015-17 to the dataset decreases the magnitude of the 30 year events by around 5%, and the 100 year events by around 10%. This is due to the period having no high intensity rainfall events. As the higher rainfall values provided by using the 1990-2015 period only are likely to lead to larger flood events this period was used for all further analysis.

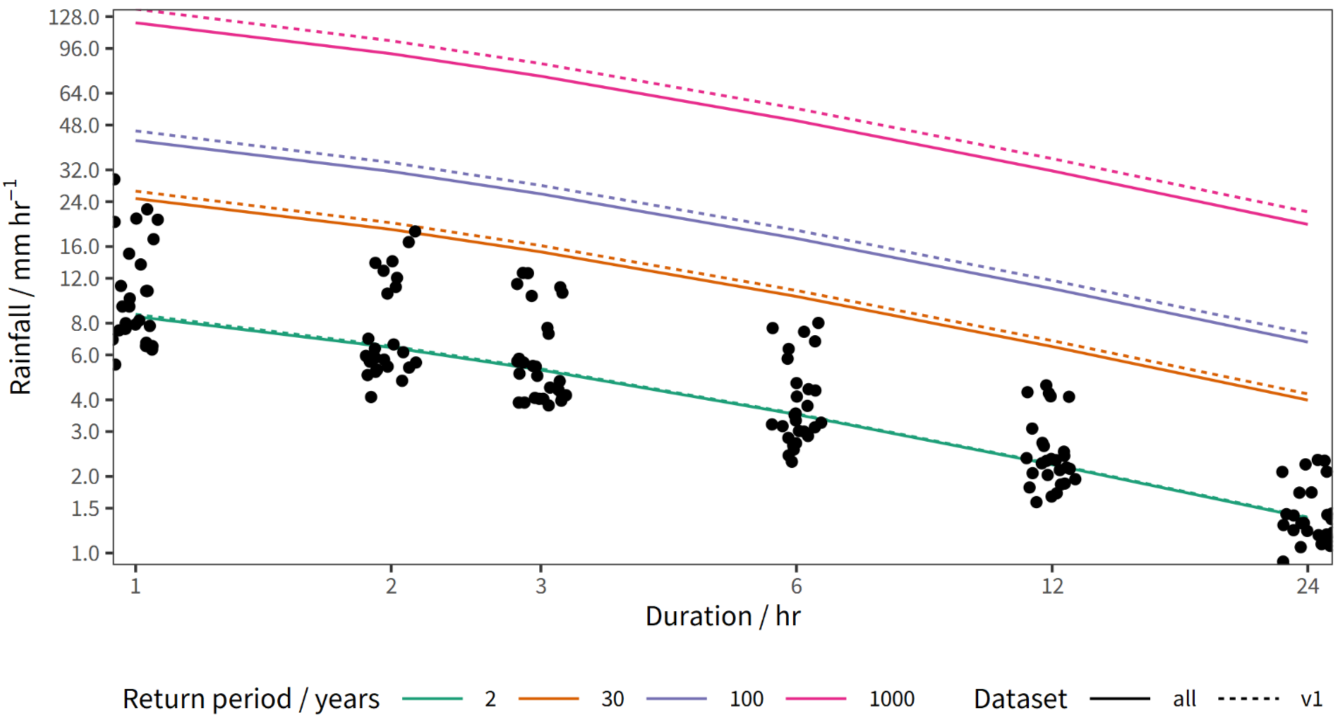

Figure 7: Intensity-Duration-Frequency curves for a variety of return periods generated from the 1990-2015 (dashed line) and 1990-2017 (solid line) rainfall datasets. Points show annual maximum intensity rainfall for 1990-2015.

4.2 Uplift due to climate change

Figure 8 shows that by 2070, it is anticipated that the intensity of same frequency events will increase by 20-25% (50% confidence), with a 95% confidence that the increase will be less than 50% on all durations and return periods. The highest uncertainty exists associated with 100 year return period events, as well as 24 hour duration events. The least uplift is anticipated to occur with shorter events (particularly 1 and 3 hour), although uncertainty is lower for 3 hour events than 1 hour events. Figure 9 shows the IDF curves with the 2070 uplift applied . In general, the intensity of 2 hour events (using 50% CI, up to 3h events if using 95% CI) could increase to approach that of 1 hour events in the present day. Alternatively, this means that the return period of rainfall events will decrease.

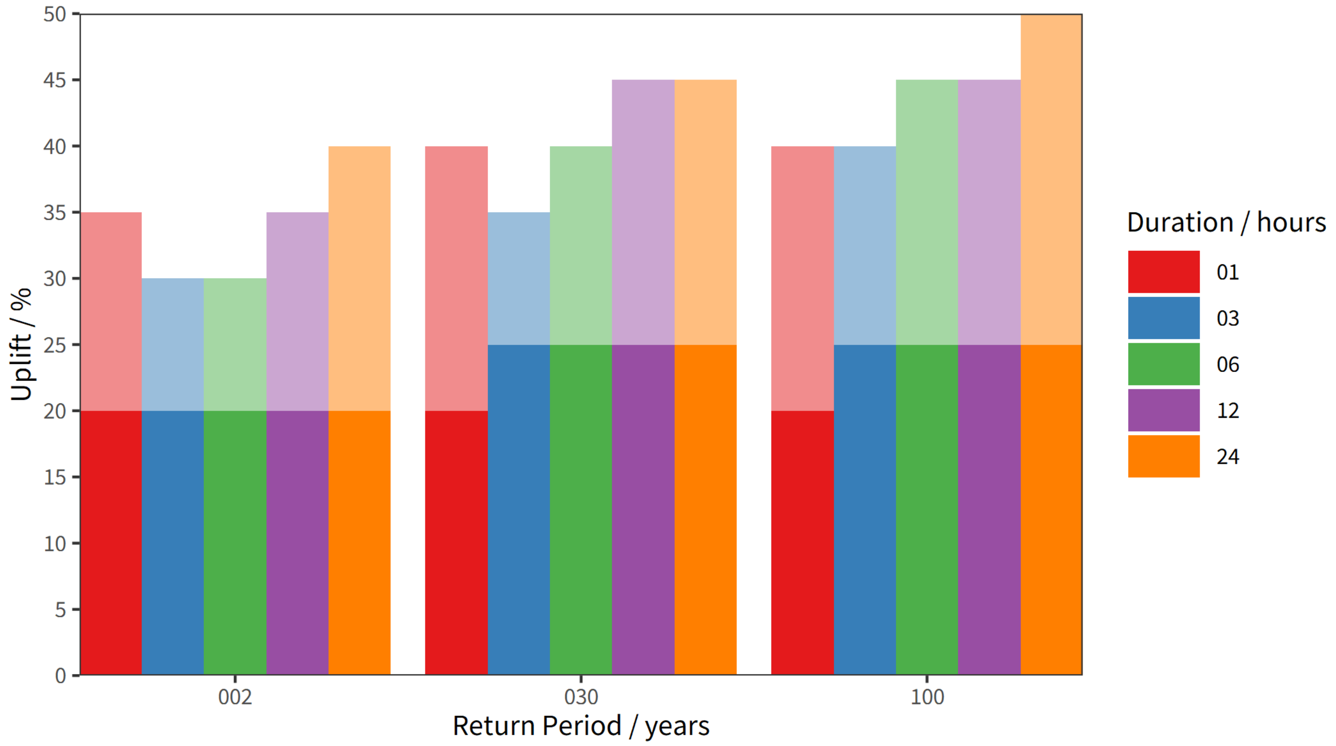

Figure 8: Percentage rainfall uplift by 2070 under the RCP8.5 scenario, derived from UKCP18 (Chan *et al.*, 2021). Lighter colours show 95% confidence, darker colours show 50% confidence.

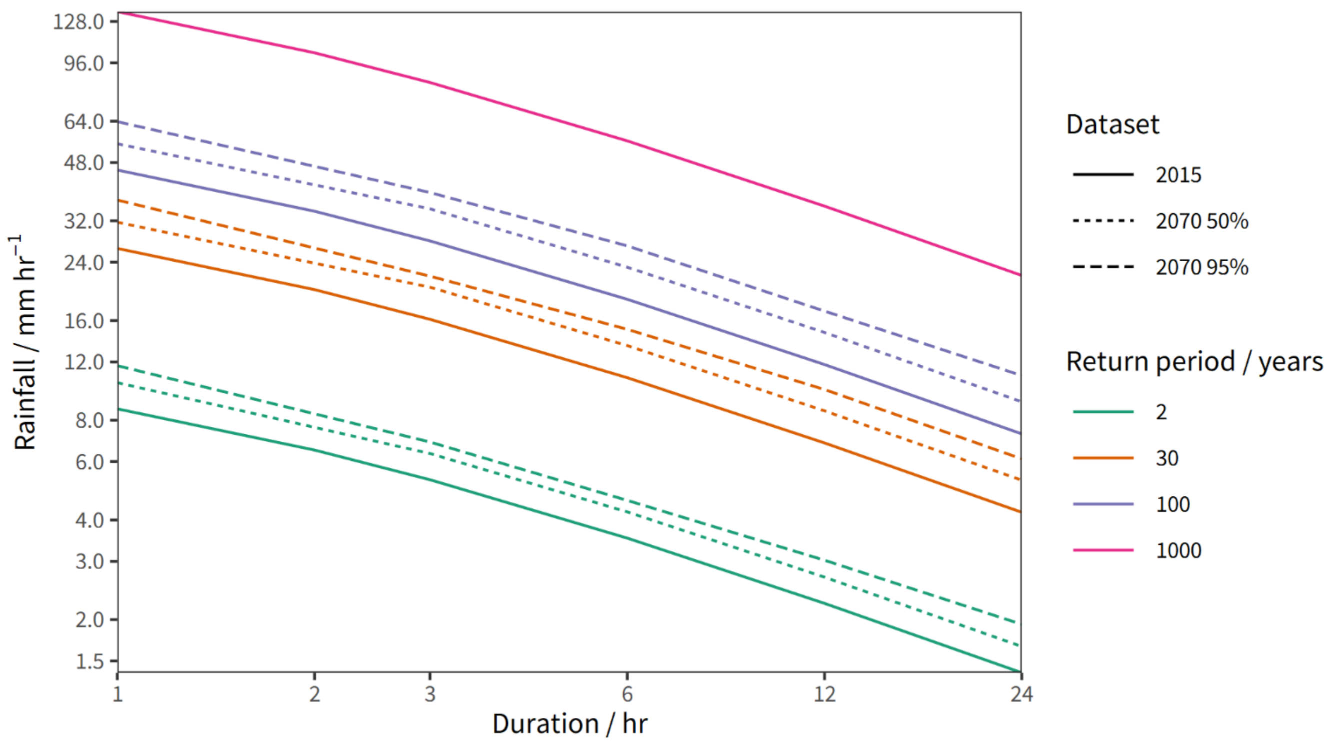

Figure 9: IDF curves with 2070 rainfall uplift (Chan *et al.*, 2021) applied, showing the 50 and 95% uplift confidence intervals.

4.3 Flood depth and extent

A strong linear correlation exists between the flood score and rainfall intensity for short duration (<6h) rainfall events, as shown in figure 10. This is particularly clear at 1 hour durations ($r^2 = 0.940$). The intensity of rainfall required to cause a flood with score of 250 decreases from 43mm/hr for a 1 hour event to 27mm/hr for a 6 hour event. The increase in flood score for a unit increase in rainfall intensity increases with duration, from 3.5:1 (1 hour) to 8.6:1 (6 hour). As only 2 datapoints are available for 2 hour events it is not possible to see a trend, although it is likely to be similar to the 1 and 3 hour events.

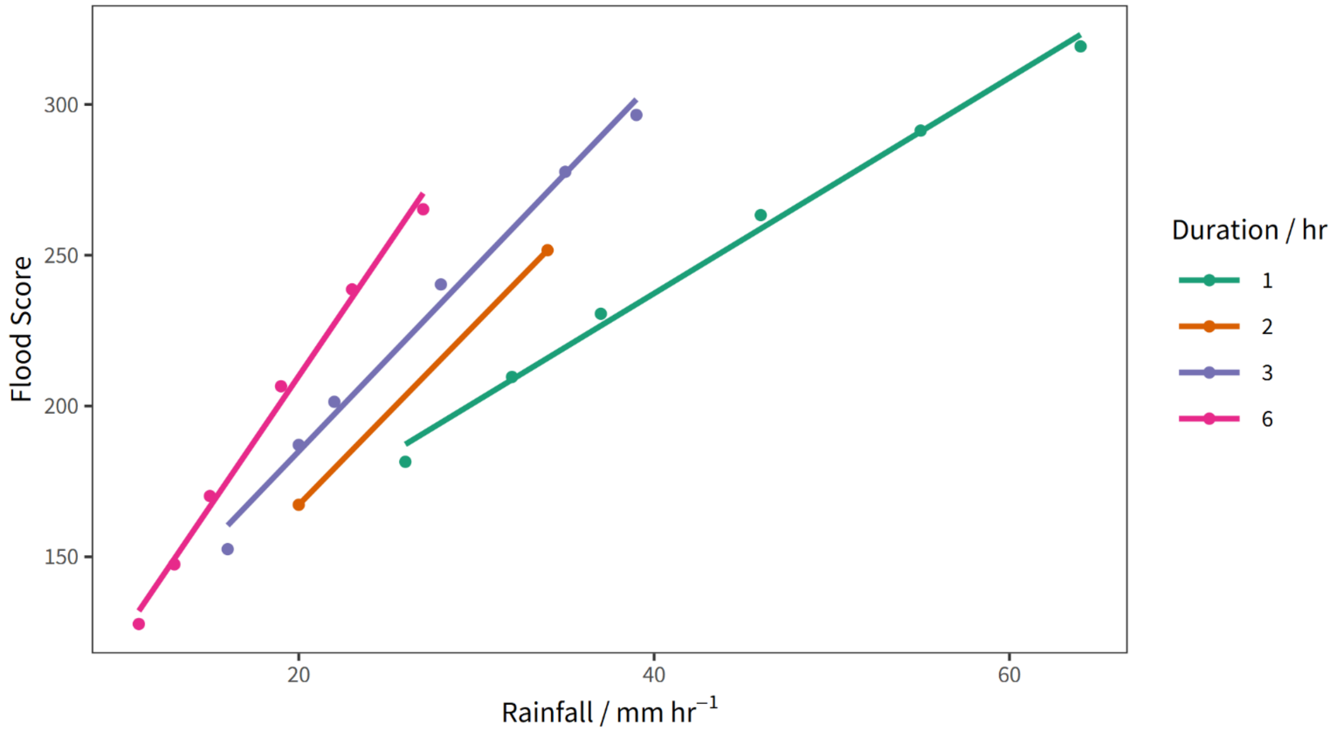

Figure 10: Correlation between Flood Score (model output) and rainfall intensity (model input), shown for short durations.

In all cases, at least 99% of the model domain is flooded to a depth of at least 0.3cm. This is likely due to the order with which model operations occur. Although not confirmed, the results suggest that during one timestep infiltration, then rainfall, then transport between cells occurs. This means that some areas with high infiltration rates and steep slopes that would otherwise have drained during the timestep actually accumulate water by the end of the timestep. This is not ideal, although it is a limitation that only really affects the lowest depth category (0.3cm). The area of high depth (100cm and 20cm) flooding is clearly linked to the duration of the storm event, with shorter but more intense events that lead to higher overall flood extent having less coverage of high depth water. This is clearly seen in the top 3 flood events in table 3; although the 2070-95-3h event has a higher flood score, and similar or greater areas of low depth (<10cm) inundation it has a 46% lower area of highest depth (>100cm) flooding.

Unsurprisingly, the rainfall events that cause the most flooding are the 100 year return period short duration future events, which have the highest intensities. However, it is notable that present day 100 year return period events (1-6h) also score relatively highly, and above many of the future longer scenarios. The 12 and 24h events do not appear to cause much flooding, even with future uplift – the 2070-95-12h event places 11th by flood score, and the 2070-95-100-24h event is at 24th. Climate change results in an increase in flood extent by an average of 8% (50% CI), although rising to 10% at the 95% CI.

One of the questions raised by table 3 is whether the flood score is most driven by flood extent or flood depth. Figure 11 shows a linear regression between area with >20cm depth (flood depth) and area with >1cm depth (flood extent), with each individual line being significant at the 1% level. A clear linear trend exists for 6, 12 and 24 hour events, although particularly for 1 hour events a non linear trend appears to exist. Interestingly, the 1 hour event's regression gradient is much closer to that of the 12 and 24 hour events than the 3 and 6 hour events, and all three appear to follow a roughly 1:4 depth:extent ratio. Thus, it can be concluded that the flood score is more strongly driven by extent than depth.

Year	CI	Return Period	Duration (hr)	Intensity (mm/hr)	Flood Score	Flood Extent / km²				
						>100cm	>20cm	>10cm	>1cm	>0.3cm
2070	95	100	1	64	319	12.4	26.1	72.1	104.3	149.5
2070	95	100	3	39	297	16.2	29.2	66.2	92.4	148.9
2070	50	100	1	55	291	9.1	21.0	65.1	98.1	149.7
2070	50	100	3	35	278	13.5	25.9	62.0	88.1	149.2
2070	95	100	6	27	265	15.2	26.9	59.2	82.0	148.8
2015		100	1	46	263	6.7	16.8	58.2	90.9	149.9
2015		100	2	34	252	8.7	19.3	56.0	83.9	149.7
2015		100	3	28	240	9.2	19.6	53.6	78.9	149.6
2070	50	100	6	23	239	11.8	22.4	53.5	75.5	149.3
2070	95	30	1	37	231	4.5	12.5	50.1	81.8	149.9
2070	95	100	12	17	211	10.6	19.7	47.4	66.6	149.3
2070	50	30	1	32	210	3.4	10.1	45.0	75.6	150.0
2015		100	6	19	207	8.2	17.1	46.4	67.4	149.7
2070	95	30	3	22	201	5.7	13.8	44.8	68.5	149.9
2070	50	100	12	15	189	8.1	16.1	42.6	61.1	149.6
2070	50	30	3	20	187	4.7	11.9	41.5	64.5	149.9
2015		30	1	26	181	2.3	7.4	38.4	66.7	150.0
2070	95	30	6	15	170	4.8	11.4	37.7	58.1	149.9
2015		30	2	20	167	2.6	7.8	36.2	60.3	150.0
2015		100	12	12	154	4.9	10.8	34.5	52.1	149.8
2015		30	3	16	153	2.6	7.4	33.3	54.6	150.0
2070	50	30	6	13	147	3.4	8.5	32.6	51.5	149.9
2015		30	6	11	128	2.4	6.1	27.9	45.7	150.0
2070	95	100	24	11	106	4.3	9.4	25.9	33.4	149.8
2070	50	100	24	9	63	2.0	4.6	16.1	20.4	150.0
2070	50	30	12	9	63	1.3	3.8	15.9	20.7	150.0
2015		100	24	7	52	1.5	3.5	13.2	16.7	150.0
2015		30	12	7	45	0.8	2.3	11.6	15.0	150.0
2070	50	30	24	5	33	0.8	2.0	8.4	10.8	150.0
2015		30	24	4	23	0.5	1.3	5.8	7.5	150.0
							Total Area			150.0

Table 3: Maximum flooded area for all rainfall scenarios using the 2020 land cover layer, sorted by descending flood score. Flood score is a composite index showing inundation area weighted by depth. The highest inundation depth for each cell is used for calculating flooded area; total area may not have been flooded at the same time. Table is ordered descending by flood score. CI shows UKCP uplift confidence interval (Chan *et al.*, 2021).

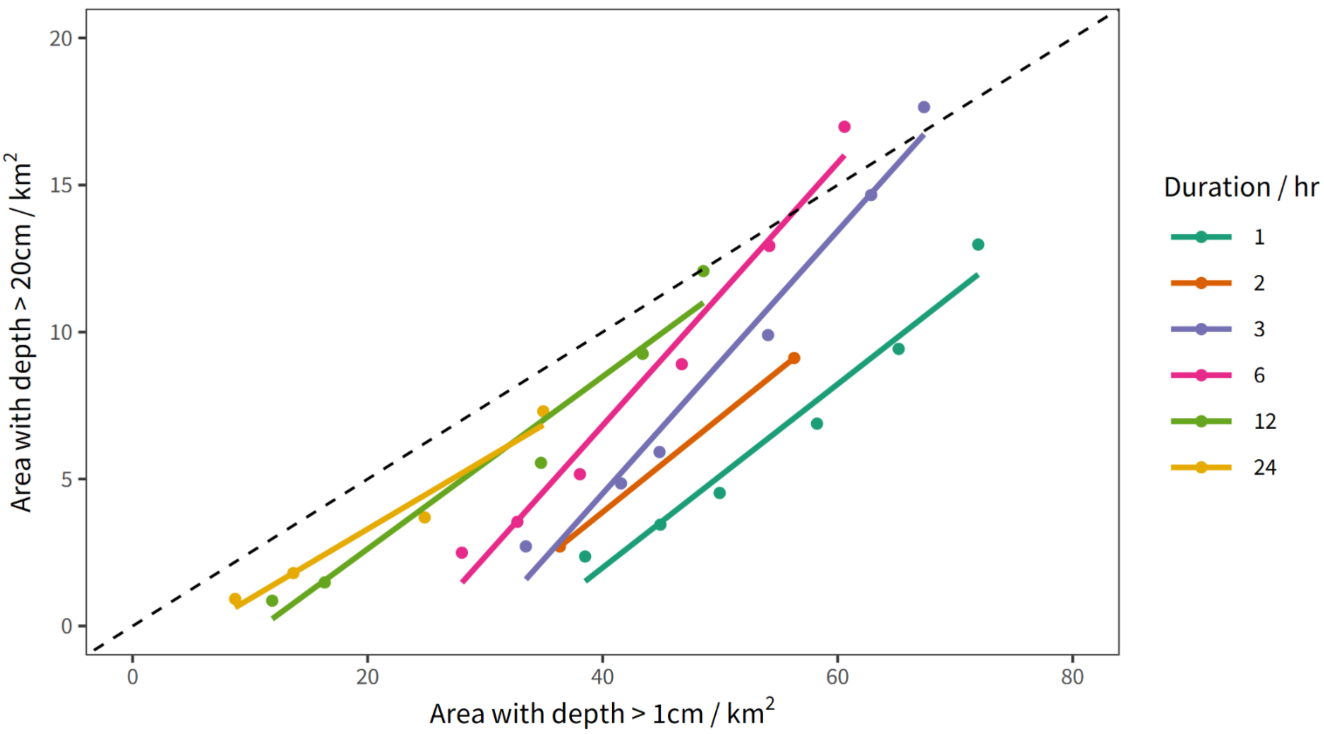

Figure 11: Correlation between flood depth and extent using depth categories; generated from model outputs. Black dashed line shows a 4:1 ratio relationship.

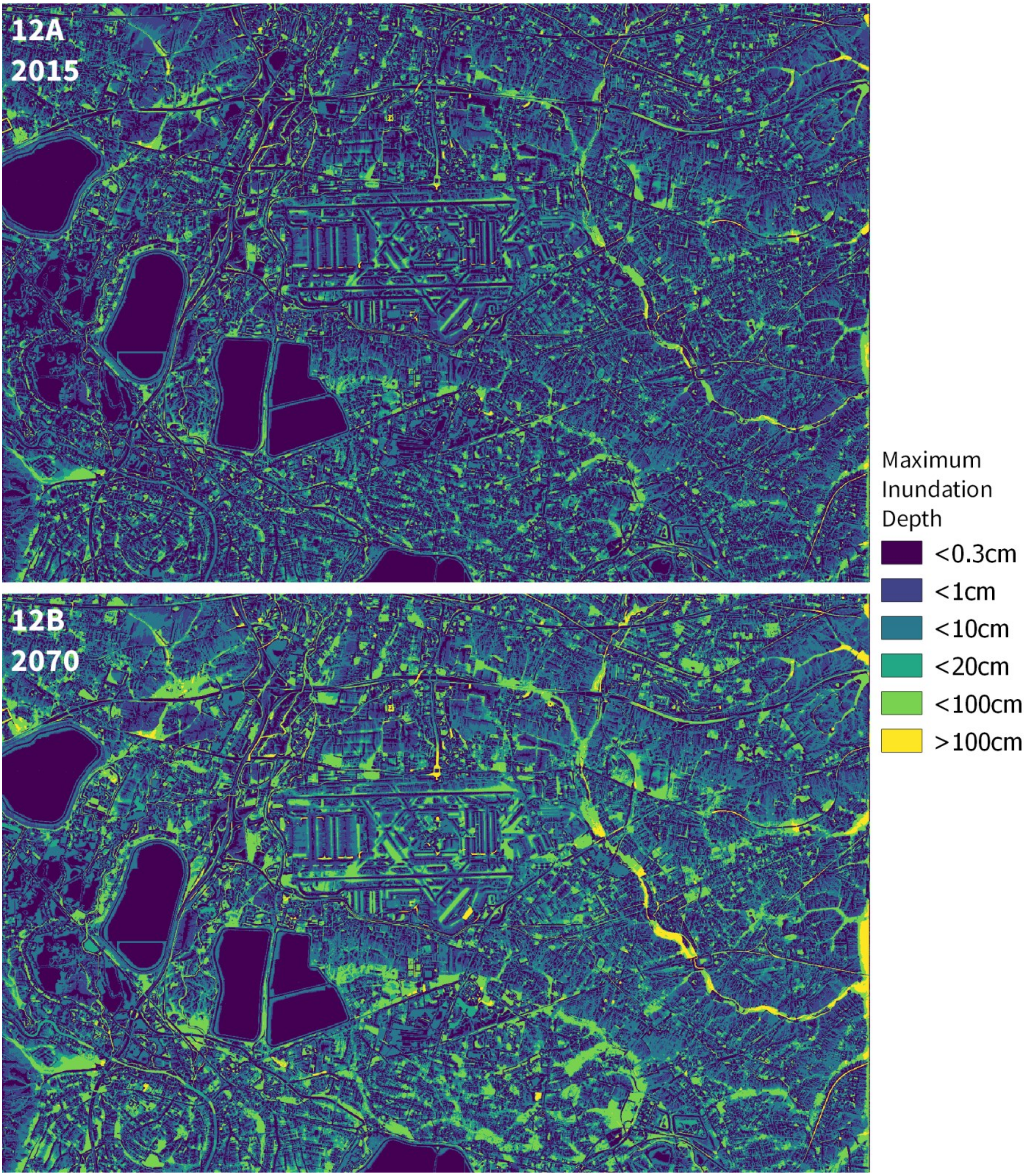

Figure 12: Maximum inundation depth (category) for each cell under all 100 year return period events for 2015 (12A) and 2070 (12B, 50% confidence rainfall uplift); generated from model outputs.

More of the airport and its surrounding areas are vulnerable to surface water flooding in 2070 (figure 12B) than the present day (figure 12A). A significant amount of >1m flooding exists in and around the River Crane to the east of the airport. This river is not classified as freshwater by the land cover map, likely due to its thick vegetation cover. This means that it was not given a high infiltration rate, allowing its valley to fill with water to depths of up to 6m in some experiments. High depths were also identified along the eastern edge of the model domain in longer simulations – this is caused by a error in the conversion of the DEM, which results in a one pixel wide 'wall' in some areas which stops water from draining over the edge. This is only seen to be an obvious issue in the 12 and 24h simulations and only affects a small (~5km^2) area of the model domain. Parts of the runways and apron around terminals 2 and 5 do not flood under any circumstances, this is due to the camber present in these areas as well as drainage. However, even in the present day widespread flooding up to a depth of 20cm is seen on the airport property, particularly in the area surrounding terminal 4, and south of terminal 5. A small area near the north entrance of the landside tunnel also floods to a depth of over 1m in 2015. This rises to over 3m in the 2070 scenario, with the whole roundabout area being inundated. Figure 12 makes clear that the flood risk in 2070 is significantly higher than 2015.

4.4 Model Sensitivity

In all cases, an increase in the drainage rate leads to a decrease in the depth of flooding, as shown in figure 13. An equal increase is also seen when drainage is removed, which implies that a linear link exists between drainage rate and the depth of flooding, at least within the range of these drainage values. Drainage has a larger impact on longer scenarios, as the drainage rate change is much larger when compared to the lower intensities of rainfall that occur on these timescales. A one way analysis of variance test was applied to investigate whether a change in the drainage rate lead to a significant difference between the flood extent at each depth category. A significant difference exists at the 1% level on all pairings except the deepest category (>100cm) using both the 1h and 6h rainfall events, although the difference tends to be larger for the 6h event than the 1h event. This is unsurprising as in general very little of the model domain is flooded to a depth above 1m, and 70% of these areas have >2m depth under the base drainage scenario, at which point an increase in drainage is unlikely to lead to a big enough reduction in depth to change category. It may be possible to further clarify this difference if raw cell depths were used rather than depth categories, although the trend seen even with discrete categories is quite clear.

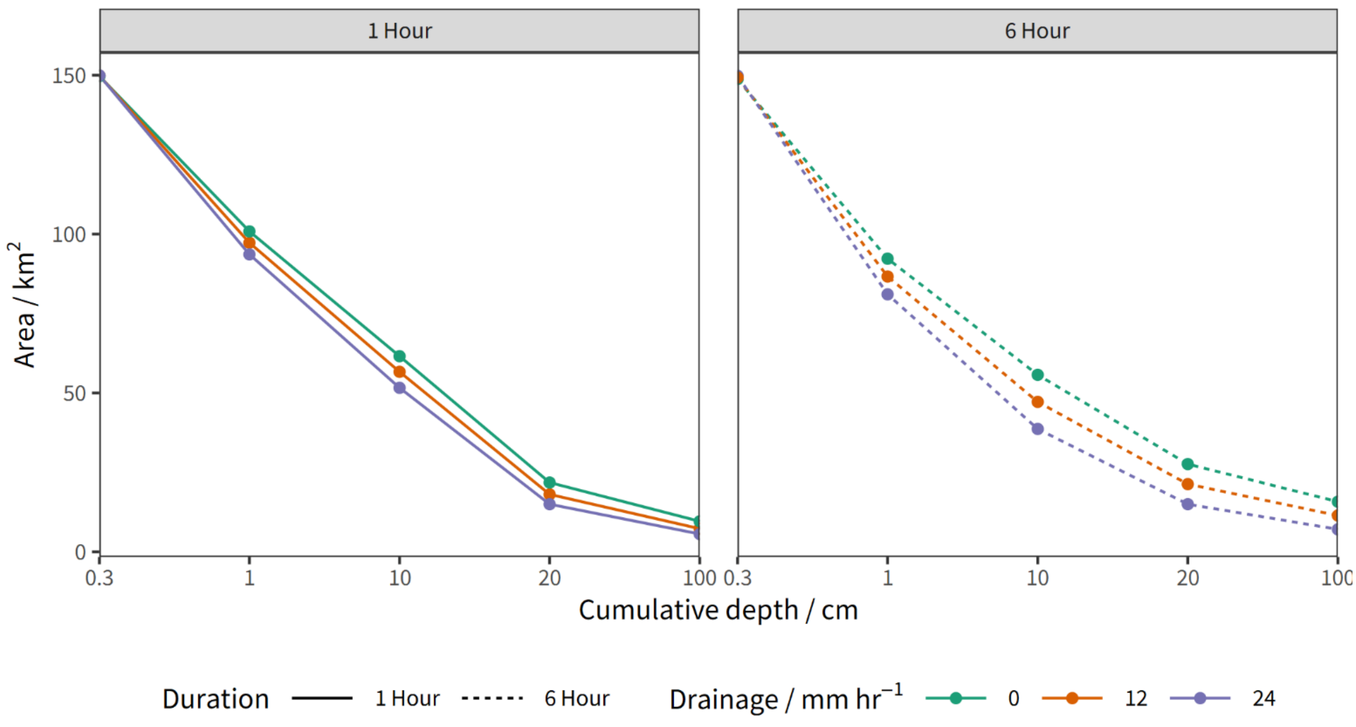

Figure 13: Cumulative flooded area at each depth for short (1 hour) and long (6 hour) duration rainfall events, with high (24mm/hr), standard (12mm/hr) and no drainage showing the sensitivity of the model to the rate of drainage applied to urban and suburban areas; generated from model outputs.

5 Discussion

5.1 Vulnerability to pluvial flooding

The results of this study make clear that there are areas of Heathrow that are vulnerable to pluvial flooding during current-day events. Most notable are the areas around tunnel entrances (airside tunnel and landside tunnel), as well as some areas around terminal 4 (south side). Additionally, the road network is at risk of flooding, notably along the south side of the airport (which connects terminal 4, cargo and logistics to the M25), the M25/M4 junction and the M4/Heathrow Central link road. The surface transportation is incredibly important to airport operations, as it is how passengers and cargo to reach the airport, as well as how important equipment (e.g. in-flight catering) reach aircraft. The effect of issues with surface transportation is quite clearly seen during snowfall events – in most cases the runways and taxiways are fairly clear, although flights are cancelled or delayed due to passenger access difficulties. It is quite clear that it would in reality not be acceptable for areas such as the landside tunnel entrance to flood under a 1 in 30 year event, which implies that a pumping or other active drainage system is likely to be present in the area. However, public information on the drainage applied is limited, so it is not possible to investigate further in this study.

5.2 Rainfall

It is clear that large amounts of variability exist in the longer timeseries rainfall events, and that there is not a clear linear trend on a decadal scale. Thus, one should be careful in assessing whether this timeseries, and the IDF curves that result from it are accurate to what may happen in the present day, as well as in the future. This is a major flaw of using a relatively short (25 year) record – the long term variability in weather patterns seen in the UK easily masks any clear trends over time, and make calculating useful return periods very difficult. Whilst it would be useful to have a longer (100+ year) timeseries, these are not currently available at a sub-daily frequencies, which makes them useless for assessing short duration, intense rainfall events. Additionally, the events that are likely to cause the most pluvial flooding may last less than an hour but have precipitation rates much higher than seen over a one hour period. It is not possible to investigate these events using the methodology of this study; a model based approach to identifying rainfall return periods may be more useful for this.

The rainfall intensities predicted as part of the IDF curves seem reasonable up to a 100 year return period, although beyond that point they are extremely unlikely to be possible. The 1h duration 1000 year return period event sits at 137mm/hr – nearly 50% higher than the highest 60 minute rainfall total recorded in the UK (110mm in 1 hour, Wheatley, 1910, (Doe, 2015, p. 270)). This is not a surprise – the extrapolation required to estimate these events is almost as intense as the rainfall they predict, when considering that only 25 years of record are provided as inputs to the IDF model. A longer timeseries would improve these predictions, although the periods available are still likely to lead to the predictions for a 1000 year return period being guesswork. The return period for longer events may also be too high – Cotterill *et al*. (2021) estimated return periods for a 50mm/day event to be in the range of 100-140 years, which would imply an average intensity of just over 2mm/hr, far less than the 7mm/hr predicted here. It may be possible to improve these results using a composite rainfall timeseries using daily data to extend the record (see (Ulrich *et al.*, 2020) for details), although this is purely academic as these events still do not produce significant pluvial flooding.

The UKCP uplift values make clear that rainfall intensities will increase in the future as a result of anthropogenic climate change. In this study, the uplift values (varying between 20 and 50%) have been applied directly to the rainfall seen on record. This approach is not ideal – the baseline used for uplift is 1970-1990, compared to our baseline of 1990-2015. The predictions are also a upper bound on what is likely to occur, as they are based on the Representative Control Pathway (RCP) 8.5 scenario, the highest used by the IPCC, representing uncontrolled emissions over the next 30 years. Thus, the 2070 rainfall scenarios provide maximum likely scenarios. A more useful way of looking at these scenarios is that events of the same magnitude will become more frequent, with 1 in 100 year events occurring approximately every 50 years. With this frequency, events that are currently outside of the range of concern will need to be mitigated against in order to sustain an appropriate risk level.

5.3 Model Sensitivity

The covered surface values are only really pertinent when considering urban and suburban areas, where they reduce the infiltration rate by 50% (suburban) or 75% (urban) respectively. For all other land cover types the effect is less than 10%, and thus negligible compared to a change in the soil base infiltration rate. The values used for urban and suburban were picked from the upper end of measurements collected by Pauleit and Duhme (2000) for environments that could be considered to be urban and suburban. They collected data in more detail than the land cover layer used for this study allows, distinguishing between types of housing (detached, terraced, multistorey), as well as types of commercial building (factory, multi-storey factory, special, construction), detail that is simply not available here. The link between the two land cover classification schemes thus depends on what is of most interest. In our case, the airport and surroundings are the core area of interest. The majority of the aerodrome is classified as urban, with some areas around the edges of taxiways being classified as *arable and horticulture*. The majority of the area classified as arable is actually covered with grass, although there are areas around the runways that are actually concrete. This error in classification is unlikely to make a particularly important effect as these areas are likely to have much higher drainage capabilities than have been used by the model.

The model is sensitive to the rate of drainage applied, which has a particular effect on both extent and depth (when considering depths <100cm). The standard drainage rate of 12mm/hr for urban and suburban areas is the middle-ground recommendation produced by the EA for urban flood models. Given the importance of the airport, and particularly the need to keep standing water to an absolute minimum to ensure aircraft operations can occur it is highly likely that much of the airside zone has significantly better drainage capabilities than a normal urban zone. The flood extent predicted by the model is extremely sensitive to the drainage rate used, although even with an upper-bound rate of 24mm/hr on urban and suburban surfaces flooding does still occur in specific zones.

5.4 Comparing our findings with other studies

Jacobs (2014) assesses the pluvial flood risk to the airport using the Risk of Flooding from Surface Water map (Environment Agency, 2019). They identify numerous areas spread widely across the airport that are at low risk of flooding, along with isolated pockets of medium and high risk. This is similar to the findings of AMEC (2014c), who state that “pockets of high risk [exist] across the wider area”, although their analysis was mostly based on review of previous reports rather than an assessment of new data. This is in line with our findings, where limited flooding - which would probably be enough to cause disruption to operations – is seen to exist throughout much of the airport (figure 12). Similarly, Jacobs (2014) identifies a high risk of surface water at the north entrance to the landside tunnel. Further, through the use of unpublished risk assessments they confirm that the airport is ‘generally protected’ from 5 year return period rainfall events, but that internal areas of buildings and extensive aerodrome zones are at risk during a 100 year return period event. This is particularly interesting, as it suggests that the approximation of drainage made in this study may even be in excess of what is seen in reality – during the most intense 100 year present day event there is a relatively limited area of the field that is flooded beyond an indoor depth of 20cm. Alternatively, higher intensity events may have been included in the risk assessments used by Jacobs (2014). They also state that the EA assumes that the capacity of water storage in the local area is at or near capacity during present-day events, and cannot be relied upon to deal with water produced by future development of the airport. The increases in intensity of storms associated with climate change is included in their assessment, although they assume that rainfall will only increase by 20%, which is in the middle of the range suggested by the UKCP18 uplift predictions (figure 8) for the RCP8.5 scenario. As a result of this, it seems fair to say that the findings of this study are similar to those of Jacobs (2014) and AMEC (2014a, 2014c), and make clear that the current drainage system is probably approaching its capacity to deal with current and future pluvial flooding.

Conclusions

This study used LISFLOOD-FP, a hydrodynamic flood model configured in this case to assess pluvial flooding to understand the risk of such flooding that the Heathrow and its surroundings face, both now and in the future. A GEV-based intensity-duration-frequency analysis was used to generate a series of extreme rainfall scenarios at the 30 and 100 year return period using a 25 year hourly rainfall grid. The results were then compared a series of reports produced for the AC in 2014 to assess the environmental risks associated with the current day airport, and future development associated with the construction of a third runway.

The use of a relatively short timeseries rainfall dataset highlights a number of issues with identifying the risk of current-day extreme events, namely the huge amount of interannual and decadal variability of the climate in the UK. This is particularly evident when looking at the period 2008-2017, where very few high intensity rainfall events occurred, whereas a large number were recorded in the preceding decade. Determining the intensity of unobserved extreme events is shown to be something of a dark art, both due to the extrapolation required and the constantly varying state of the climate. This is compounded by anthropogenic climate change, which is shown to result in significant increases in the intensity and frequency of rainstorms.

In the present day, the airport is shown to be generally at low risk of pluvial flooding, both by this study and Jacobs (2014). However, notable areas of higher risk exist, such as the northern entrance to the landside tunnel. This study identifies somewhat smaller risks in the present day than Jacobs (2014), which is likely due to different modelling assumptions. Nethertheless, this study corroborates the findings of both Jacobs (2014) and AMEC (2014a, 2014c), and suggests that pluvial flooding has the potential to be a major issue for the airport in the future.

The hydrodynamic flood model used in this study is shown to be somewhat sensitive to the rate of drainage applied. This is particularly true in urban and suburban areas, and unsurprising as the drainage rate far exceeds the background infiltration rate in these areas. This is a significant challenge for any pluvial model, especially where complex drainage systems are present. This study suggests that a strong reliance on these drainage systems exists at the airport, and that upgrades in their capabilities may be needed in the future to deal with future climate change.

References

AMEC (2014a) *Heathrow's North-West Runway: Assessment of Flood Risk*. AMEC Environment and Infrastructure UK Limited. Available at: https://www.heathrow.com/content/dam/heathrow/web/common/documents/company/about/airports-commission/technical-assessment/06_Heathrow_3RNW_-_Assessment_of_Flood_Risk.pdf.

AMEC (2014b) *Heathrow's North-West Runway: Water Quality and Hydro-ecology Assessment*. AMEC Environment and Infastructure UK Limited. Available at: https://www.heathrow.com/content/dam/heathrow/web/common/documents/company/about/airports-commission/technical-assessment/05_Heathrow_3RNW_-_Water_Quality_and_Hydro-ecology_Assessment.pdf.

Bates, P.D. *et al.* (2005) 'Numerical Modelling of Floodplain Flow', in Bates, Paul D., Lane, S.N., and Ferguson, R.I. (eds) *Computational Fluid Dynamics*. Chichester, UK: John Wiley & Sons, Ltd, pp. 271–304. doi:10.1002/0470015195.ch11.

Bates, P.D. and De Roo, A.P.J. (2000) 'A simple raster-based model for flood inundation simulation', *Journal of Hydrology*, 236(1–2), pp. 54–77. doi:10.1016/S0022-1694(00)00278-X.

Bates, P.D., Horritt, M.S. and Fewtrell, T.J. (2010) 'A simple inertial formulation of the shallow water equations for efficient two-dimensional flood inundation modelling', *Journal of Hydrology*, 387(1–2), pp. 33–45. doi:10.1016/j.jhydrol.2010.03.027.

Batjes, N.H. *et al.* (2017) 'WoSIS: providing standardised soil profile data for the world', *Earth System Science Data*, 9(1), pp. 1–14. doi:10.5194/essd-9-1-2017.

BBC News (2021) 'Covid: Heathrow to trial fast-tracking vaccinated arrivals', *BBC News*, 7 July. Available at: https://www.bbc.com/news/business-57743038 (Accessed: 6 April 2022).

CAA (2020a) *Annual airport data 2019*. Civil Aviation Authority. Available at: https://www.caa.co.uk/data-and-analysis/uk-aviation-market/airports/uk-airport-data/uk-airport-data-2019/annual-2019/ (Accessed: 31 March 2022).

CAA (2020b) *New contaminated runway reporting system*, *Civil Aviation Authority*. Available at: https://www.caa.co.uk/commercial-industry/airports/safety/runways/new-contaminated-runway-reporting-system/ (Accessed: 30 March 2022).

Chan, S.C. *et al.* (2021) 'Extreme precipitation return level changes at 1, 3, 6, 12, 24 hours for 2050 and 2070, derived from UKCP Local Projections on a 5km grid for the FUTURE-DRAINAGE Project'. NERC EDS Centre for Environmental Data Analysis. Available at: https://catalogue.ceda.ac.uk/uuid/18f83caf9bdf4cb4803484d8dce19eef (Accessed: 20 January 2022).

Doe, R.K. (2015) *Extreme Weather: Forty Years of the Tornado and Storm Research Organisation (TORRO)*. Hoboken, UNITED KINGDOM: John Wiley & Sons, Incorporated. Available at: http://ebookcentral.proquest.com/lib/bristol/detail.action?docID=4334738 (Accessed: 5 April 2022).

Environment Agency (2019) 'What is the Risk of Flooding from Surface Water Map?', 2. Available at: https://assets.publishing.service.gov.uk/government/uploads/system/uploads/attachment_data/file/842485/What-is-the-Risk-of-Flooding-from-Surface-Water-Map.pdf.

Environment Agency (2020) *Flood and coastal erosion risk management report: 1 April 2019 to 31 March 2020*. Available at: https://www.gov.uk/government/publications/flood-and-coastal-risk-management-national-report/flood-and-coastal-erosion-risk-management-report-1-april-2019-to-31-march-2020 (Accessed: 25 March 2022).

Environment Agency (2021a) *LIDAR Composite DTM 2020 - 1m*. Available at: https://data.gov.uk/dataset/b1ff0a9c-74d3-4b97-a3fb-c8ab39ef6152/lidar-composite-dtm-2020-1m (Accessed: 3 March 2022).

Environment Agency (2021b) *Real time flood monitoring data: Archives*. Available at: https://environment.data.gov.uk/flood-monitoring/archive (Accessed: 15 January 2022).

Golding, B., Clark, P. and May, B. (2005) 'The Boscastle flood: Meteorological analysis of the conditions leading to flooding on 16 August 2004', *Weather*, 60(8), pp. 230–235. doi:10.1256/wea.71.05.

Graham, P. (2013) 'Airports Commission Stakeholder Briefing', in. Available at: https://assets.publishing.service.gov.uk/government/uploads/system/uploads/attachment_data/file/88322/130220-airport-commission-briefing.pdf.

Horritt, M.S. and Bates, P.D. (2002) 'Evaluation of 1D and 2D numerical models for predicting river flood inundation', *Journal of Hydrology*, 268(1), pp. 87–99. doi:10.1016/S0022-1694(02)00121-X.

Hunter, N.M. *et al.* (2005) 'An adaptive time step solution for raster-based storage cell modelling of floodplain inundation', *Advances in Water Resources*, 28(9), pp. 975–991. doi:10.1016/j.advwatres.2005.03.007.

Jacobs UK (2014) *Water and flood risk: Baseline*. Airports Commission. Available at: https://www.gov.uk/government/publications/additional-airport-capacity-water-and-flood-risk-analysis.

JBA Risk Management (2021) *A retrospective look at summer 2021 London flash floods*. Available at: https://www.jbarisk.com/flood-services/event-response/a-retrospective-look-at-summer-2021-london-flash-floods/ (Accessed: 25 March 2022).

Leon, D.C. *et al.* (2016) 'The Convective Precipitation Experiment (COPE): Investigating the Origins of Heavy Precipitation in the Southwestern United Kingdom', *Bulletin of the American Meteorological Society*, 97(6), pp. 1003–1020. doi:10.1175/BAMS-D-14-00157.1.

Lewis, E. *et al.* (2019) 'Gridded estimates of hourly areal rainfall for Great Britain 1990-2014 [CEH-GEAR1hr]', *NERC EDS Environmental Information Data Centre* [Preprint]. doi:10.5285/d4ddc781-25f3-423a-bba0-747cc82dc6fa.

Lewis, E. *et al.* (2022) 'Gridded estimates of hourly areal rainfall for Great Britain 1990-2016 [CEH-GEAR1hr] v2', *NERC EDS Environmental Information Data Centre* [Preprint]. doi:10.5285/fc9423d6-3d54-467f-bb2b-fc7357a3941f.

Lowe, J.A. *et al.* (2018) *UKCP18 Science Overview Report*. Available at: https://www.metoffice.gov.uk/pub/data/weather/uk/ukcp18/science-reports/UKCP18-Overview-report.pdf.

Met Office (2022) *Met Office Integrated Data Archive System (MIDAS) Land and Marine Surface Stations Data (1853-current)*. NCAS British Atmospheric Data Centre. Available at: https://catalogue.ceda.ac.uk/uuid/220a65615218d5c9cc9e4785a3234bd0 (Accessed: 3 April 2022).

Met Office Hadley Centre (2019) ‘UKCP18 Convection-Permitting Model Projections for the UK at 2.2km resolution’, *NERC EDS Centre for Environmental Data Analysis* [Preprint]. Available at: http://catalogue.ceda.ac.uk/uuid/ad2ac0ddd3f34210b0d6e19bfc335539 (Accessed: 18 February 2022).

Morton, R.D. *et al.* (2021) ‘Land Cover Map 2020 (10m classified pixels, GB)’, *NERC EDS Environmental Information Data Centre* [Preprint]. doi:https://doi.org/10.5285/35c7d0e5-1121-4381-9940-75f7673c98f7.

Naso, S. *et al.* (2016) ‘A novel approach to flood risk assessment: the Exposure-Vulnerability matrices’, *E3S Web of Conferences*. Edited by M. Lang, F. Klijn, and P. Samuels, 7. doi:10.1051/e3sconf/20160708007.

Neal, J., Schumann, G. and Bates, P. (2012) ‘A subgrid channel model for simulating river hydraulics and floodplain inundation over large and data sparse areas: FLOODPLAIN INUNDATION OVER LARGE AREAS’, *Water Resources Research*, 48(11). doi:10.1029/2012WR012514.

Pregnolato, M. *et al.* (2017) ‘The impact of flooding on road transport: A depth-disruption function’, *Transportation Research Part D: Transport and Environment*, 55, pp. 67–81. doi:10.1016/j.trd.2017.06.020.

Sacramento County (1990) ‘14.10.110 Soil Infiltration Rates’, in *Sacramento County Code*. Available at: http://qcode.us/codes/sacramentocounty/view.php?topic=14-14_10-14_10_110 (Accessed: 28 January 2022).

Sampson, C.C. *et al.* (2013) ‘An automated routing methodology to enable direct rainfall in high resolution shallow water models’, *Hydrological Processes*, 27(3), pp. 467–476. doi:10.1002/hyp.9515.

van der Sande, C.J., de Jong, S.M. and de Roo, A.P.J. (2003) ‘A segmentation and classification approach of IKONOS-2 imagery for land cover mapping to assist flood risk and flood damage assessment’, *International Journal of Applied Earth Observation and Geoinformation*, 4(3), pp. 217–229. doi:10.1016/S0303-2434(03)00003-5.

Sayers, P.B. *et al.* (2020) *Third UK Climate Change Risk Assessment (CCRA3): Future flood risk*. 3. Committee on Climate Change. Available at: https://www.ukclimaterisk.org/wp-content/uploads/2020/07/Future-Flooding-Main-Report-Sayers-1.pdf (Accessed: 31 March 2022).

Sharman, L. and Burford, R. (2021) ‘London floods: Hospitals and DLR station hit as streets turn to rivers’, *Evening Standard*, 26 July. Available at: https://www.standard.co.uk/news/london/london-flash-floods-rain-and-thunderstorms-b947578.html (Accessed: 25 March 2022).

Smith, H. (2011) ‘Replacement DLR station at Pudding Mill Lane approved’, *Global Railway Review*. Available at: https://www.globalrailwayreview.com/news/10031/replacement-dlr-station-at-pudding-mill-lane-approved-and-will-enable-crossrail-tunnelling-works-to-proceed/ (Accessed: 31 March 2022).

Ulrich, J. *et al.* (2020) ‘Estimating IDF Curves Consistently over Durations with Spatial Covariates’, *Water*, 12(11). doi:10.3390/w12113119.

Ulrich, J. *et al.* (2022) *IDF: Estimation and Plotting of IDF Curves*. Available at: https://CRAN.R-project.org/package=IDF (Accessed: 30 March 2022).

Watts, G. *et al.* (2015) ‘Climate change and water in the UK – past changes and future prospects’, *Progress in Physical Geography: Earth and Environment*, 39(1), pp. 6–28. doi:10.1177/0309133314542957.

University of Bristol Research Ethics Application

Investigator information

Application Submitter Details

Title

Mx

First Name

Alexander

Surname

Beavil

Faculty

Faculty of Science

Department

School of Geographical Sciences

School

School of Geographical Sciences

Telephone

Email

alexander.beavil.2019@bristol.ac.uk

Preferred Name or Also Known As

Alex Beavil

Faculty

Science

School / Department / Centre

School of Geographical Sciences

Please select the Research Ethics Committee (REC) to review your research ethics application:

School of Geographical Sciences Research Ethics Committee

Is this a student project? (I.e. Is the ethics application submitted as part of your student qualification?)

Yes

Please declare your level of study

Undergraduate

Supervisor Contact Details

Title

Dr

First Name

Jeffrey

Surname

Neal

Department

Physical Geography

Faculty

Faculty of Science

Email

J.Neal@bristol.ac.uk

Supervisor Details (if external to the University of Bristol)

Please provide their name, organisation details, email address and telephone number.

Please provide details of any other researchers/collaborators involved in the study.

To proceed to the next page select 'Next' in the Actions tiles.

To save your application for completion and submission at a later date please select 'Save' in the Actions tiles.

Brief study outline

Brief Project Outline (up to approximately 300 words)

Heathrow Airport is the UK's largest airport, handling over 80 million passengers in 2019, and as such one of the largest areas of impermeable surfaces in the country. The airport also sits between the floodplains of the River Colne, Crane and human modified Longford and Duke of Northumberland's rivers, with part of the airport within the 1 in 1000 year flood zone. Whilst there is little past evidence of flooding on the airfield itself, there is a long history of extensive flooding to the west and east of the airport. Additionally, the underlying geology (River Terrace Gravels) leads to groundwater levels being very close to the surface. As such, in this project I will use the LISFLOOD-FP model to run a series of simulations to understand the effect of the airport's impermeable surfaces on the local flood risk. Specifically, I will look at the current-day risk associated with the 2020 airport layout as well as the change in risk associated with anticipated climate change by 2085. I will also perform a series of speculative experiments based on of the airport did not exist (no impermeable surfaces) as well as changes to the airport layout associated with the preferred Heathrow expansion plan.

To proceed to the next page select 'Next' in the Actions tiles.

To save your application for completion and submission at a later date please select 'Save' in the Actions tiles.

Checklist questions

Checklist Questions Does your research involve any of the following? Tick all that apply

The following list is the standard University Checklist of common areas of ethical concern. If your research involves any of these issues you must ensure that you expand upon them in the sections that follow and if you are an inexperienced researcher (undergraduate/ taught masters) you are unlikely to receive a favourable ethical opinion.

- [ ] Participants who are particularly vulnerable or unable to give informed consent

  * Examples of vulnerable participants are children, people with learning difficulties, patients, people experiencing emotional distress or mental illness, people living in care or nursing homes, and people recruited through self-help groups, participants in a dependent or unequal relationship with the researcher(s) or research supervisor.

- [ ] Participants to take part without their knowledge and consent at the time

  * Examples include the covert observation of people or incidental recording of others.

- [ ] Actively deceiving participants

  * Examples include deliberately falsely informing participants, withholding information from participants or misleading participants in such a way that they are likely to object or show unease when debriefed about the study.

- [ ] Discussion or collection of information on sensitive topics or considered special category status under GDPR

  * Special Category Status under GDPR include:

  - personal data revealing racial or ethnic origin;
  - personal data revealing political opinions;
  - personal data revealing religious or philosophical beliefs;
  - personal data revealing trade union membership;
  - genetic data;
  - biometric data (where used for identification purposes);
  - data concerning health;
  - data concerning a person's sex life;
  - and data concerning a person's sexual orientation.

  If the research is in relation to any of the sensitive topics listed then the legal issue requiring such scrutiny in such cases that 'explicit consent' must be obtained and the consenting process reviewed by the ethics committee

- [ ] Invasive procedures

  * Invasive procedures may include:

  - Administration of drugs placebos:
  - Other substances (e.g., drinks, foods, food or drink constituents, dietary supplements) to study participants;
  - Biological samples from participants be obtained;
  - Pain or more than mild discomfort likely to result from the study.

- [ ] Scans (e.g. MR, CT, PET) or x-rays of research participants

- [ ] Photographs, videoing, recording or similar of research participants without their consent

- [ ] Financial inducement (other than reasonable expenses and compensation for time)

- [ ] The use or storage of information about living people whose personal identity could be discovered from that information

- [ ] Funds received from politically or culturally sensitive funding sources

  *Examples include the defence sector, projects with potential environmental effects and other internationally regulated or protected industries. For more information, please follow the link to the 'Research Governance and Integrity Policy'

- [x] None of the above

To proceed to the next page select 'Next' in the Actions tiles.

To save your application for completion and submission at a later date please select 'Save' in the Actions tiles.

Study design and background

Geographical Sciences Ethics Application Form

All dissertation projects require a completed, reviewed and approved ethics application. In order for your research ethics application to be reviewed by your supervisor and Geography's Ethics Committee, you must complete all elements of the form and ensure that all relevant documentation has been uploaded.

Is this a multi-stage ethics application? (eg Are you seeking ethics approval for an initial stage of your project and will seek further approvals when required.)

- ☐ Yes
- ☑ No

Methods - Tick any of the methods you are proposing to carry out. Tick all that apply.

- ☐ Methods that involve human participants
- ☐ Archival methods and/or qualitative secondary data e.g. text or images
- ☐ Analysis of quantitative secondary data
- ☑ Numerical modelling
- ☐ Field and/or laboratory work

What is the copyright status of the model/software you will use?

The model and/or software I plan to use is open access e.g. Creative Commons

Specify what model or software you will be using and why no copyright restrictions for its use exists. Provide the URL to substantiate this where appropriate.

LISFLOOD-FP
https://zenodo.org/record/4073011#.YCrpMGj7Q2w
GPL v3 license
Land cover maps
https://catalogue.ceh.ac.uk/documents/b3dfc4c7-c9bd-4a02-bed8-46b2a41be04a
License at https://eidc.ceh.ac.uk/licences/lcm-raster/plain
LIDAR/elevation
https://data.gov.uk/dataset/b1ff0a9c-74d3-4b97-a3fb-c8ab39ef6152/lidar-composite-dtm-2020-1m
Open Government License v3 - https://www.nationalarchives.gov.uk/doc/open-government-licence/version/3/
QGIS
https://www.qgis.org/en/site/forusers/download.html
GPL V2 - https://github.com/qgis/QGIS/blob/master/doc/LICENSE
UKCP rainfall data
https://ukclimateprojections-ui.metoffice.gov.uk/products
OGL v3

Is this research funded?

No

Do you or your supervisor(s) have any actual or potential conflict of interest in this study?

No

Research outputs

How will the results of your study be disseminated?

Resulting documents, notably the final dissertation report, may be shared to GitHub and my web services (including my personal website, https://aeroniemi.com) in LaTeX and html/pdf form only. No source data will be redistributed.

Please outline how you will undertake this research with good research integrity principles in place.

The data presented in the final report will be derivative only, and not include raw initial datasets. initial datasets will be used in line with the conditions of their license, with particular note to the CEH land cover dataset, which have the most restrictive license of all used data and software. Clear definitions for each model run, and chart content will be presented as part of figure legends/appendices as appropriate. Additionally, as the project focuses on the findings of the 2015 Airport's Commission reports, strong effort will be made to ensure that the results of my project reflect the datasets and model that is being used, rather than the Airport's Commission's findings.

Supporting Information

Supporting information Please provide any additional information in relation to your study that you think may be relevant.

N/A

Any other information Please upload any other documents that you think may be relevant to your research.

To proceed to the next page select 'Next' in the Actions tiles.

To save your application for completion and submission at a later date please select 'Save' in the Actions tiles.

Signatures

Supervisor Signature

Once you have completed your ethics form and uploaded all related documents ask your supervisor to review your ethics application by clicking this button.

Signed: This form was signed by Dr Jeffrey Neal (J.Neal@bristol.ac.uk) on 11/11/2021 12:15